



Linköping University
INSTITUTE OF TECHNOLOGY

Prediction and Modelling of Fastener Flexibility Using FE

Freddie Gunbring

Solid Mechanics

Degree Project

Department of Management and Engineering

LIU-IEI-TEK-A--08/00368--SE

Abstract

This report investigates the feasibility and accuracy of determining fastener flexibility with 3D FE and representing fasteners in FE load distribution models with simple elements such as springs or beams. A detailed study of 3D models compared to experimental data is followed by a parametric study of different shell modelling techniques. These are evaluated and compared with industry semi-empirical equations.

The evaluated 3D models were found to match the experimental values with good precision. Simulations based on these types of 3D models may replace experimental tests. Two different modelling techniques were also evaluated for use in load distribution models. Both were verified to work very well with representing fastener installations in lap-joints using the ABAQUS/Standard solver. Further improvement of one of the models was made through a modification scale factor. Finally, the same modelling technique was verified using the NASTRAN solver.

To summarize, it is concluded that:

- Detailed 3D-models with material properties defined from stress-strain curves correspond well to experiments and simulations may replace actual flexibility tests.
- At mid-surface modelling of the connecting parts, beam elements with a circular cross section as a connector between shell elements is an easy and accurate modelling technique, with the only data input of bolt material and dimension.
- Using connector elements is accurate only if the connecting parts are modelled in the same plane, i.e. with no offset. Secondary bending due to offset should only be accounted for once and only once throughout the analysis, and it is already included in the flexibility input.

Sammanfattning

Den här rapporten undersöker möjligheten och noggrannheten i att prediktera fästelementsflexibilitet med hjälp av 3D FE samt att representera fästelement i FE lastfördelningsmodeller med enkla element, exempelvis fjädrar eller balkar. En detaljerad studie av 3D modeller som jämförs med experimentella värden följs av en parameterstudie av olika skalmodelleringsstekniker. Dessa utvärderas och jämförs även med semi-empiriska formler som normalt används inom flygindustrin.

De utvärderade 3D modellerna matchar experimentella värden med god precision. Simuleringar baserade på dessa typer av 3D modeller kan ersätta liknande experimentellt arbete. Två olika modelleringsstekniker utvärderades med avseende på användning i lastfördelningsmodeller. Båda verifierades som fungerande vid representering av fästelementinstallationer i bultförband med användning av beräkningsprogrammet ABAQUS/Standard. Ytterligare förbättring uppnåddes genom en skalfaktorsmodifiering av indata. Slutligen verifierades modelleringsstekniken med gott resultat för det ofta använda beräkningsprogrammet NASTRAN.

Följande slutsatser kan dras:

- Detaljerade 3D modeller med materialegenskaper definierade från spänning - töjnings diagram stämmer bra med experimentella värden och liknande prov kan ersättas med simuleringar.
- Vid modellering i medelytan av plattorna är balkelement med cirkulärt tvärsnitt som en koppling mellan skalelement en enkel och bra modelleringssteknik, med endast indata i form av bultmaterial och dimension.
- Att använda connectorelement är endast användbart när plattorna modelleras i samma plan, det vill säga utan offset. Sekundär böjning ska bara tas i beaktning en gång i analysen som helhet, och det är redan inkluderat i ingångsvärdet för flexibilitet.

Preface

This report marks the end of the author's studies at the Linköping University. It is the final assignment towards the degree of Master of Science in Mechanical Engineering. The work for the project "Prediction and Modelling of Fastener Flexibility using FE" has been conducted at Saab Aerostructures in Linköping, Sweden, during the autumn of the year 2007.

The author would like to thank Anders Bredberg for his invaluable support and guidance throughout this project. Many thanks must also be pointed towards the rest of the engineering staff at Saab Aerostructures, for their input and suggestions.

This report is based on independent work by the author. Any contribution from other sources are acknowledged and referenced where appropriate.

Freddie Gunbring, Linköping 2008

Contents

Abstract	iii
Sammanfattning	iv
Preface.....	v
Figures.....	viii
Tables.....	ix
Notation and units	x
1 Introduction	1
1.1 Objective	1
1.2 Background	1
1.3 Procedure.....	3
2 Determination of bolt flexibility using detail FE.....	4
2.1 FE-model.....	4
2.1.1 General definition	4
2.1.2 Defining contact.....	5
2.1.3 Defining friction.....	6
2.1.4 Defining material properties	6
2.1.5 Using pre-tension	7
2.2 Verification of 3D-model with experiments	9
2.2.1 Measurement definition of specimens	9
2.2.2 Results.....	12
2.3 Comparison with empirical equations.....	18
2.4 Conclusions	20
3 Modelling technique - Load distribution models	21
3.1 FE-model.....	21
3.1.1 Beam Element Method	22
3.1.2 Connector Element Method	22
3.2 Parametric study.....	22
3.2.1 Results.....	23
3.2.2 Load distribution in 3-bolted model	27
3.3 Modifying factor for radius input.....	29
3.4 Interfacing with NASTRAN solver.....	32
4 Conclusions and Discussion	33
4.1 Recommendations and guidelines.....	34
5 Further work	35
References.....	36

Figures

Figure 1.1 – Typical analysis and design procedure.....	1
Figure 2.1 – Full view of 3D model.....	4
Figure 2.3 – Definition of master and slave surfaces.....	5
Figure 2.2 – Zoomed view of fine mesh	5
Figure 2.4 – Stress strain curve (full range) for Al 2024-T3 (MIL-HDBK-5E).....	6
Figure 2.5 – Stress strain curve (full range) for Ti 6Al4V (MMPDS-02)	7
Figure 2.6 – Load decay for Hi-Lok fasteners (Huckcomp, 1991).....	8
Figure 2.7 – Specimen IISS06	9
Figure 2.8 – Specimen IDS01	9
Figure 2.9 – Geometry definition for single shear joints	10
Figure 2.10 – Geometry definition for double-shear joints	10
Figure 2.11 – Measurement definition for single-shear lap-joint	11
Figure 2.12 – Measurement definition for double-shear lap-joint	11
Figure 2.13 – Zoomed section of elastic ISS11 specimen	13
Figure 2.14 – Elastic model with pre-tension 6300 N, without friction	13
Figure 2.15 – Effect of pre-tension parameter, no friction used	14
Figure 2.16 – Effect of friction parameter, with plasticity and pre-tension 6300 N	14
Figure 2.17 – ISS11 plasticity model with pre-tension 6300 N and friction coefficient 0.3 ..	15
Figure 2.18 – IISS06 elastic model with pre-tension 500 N, without friction	15
Figure 2.19 – IISS06 plasticity model with pre-tension 500 N and friction coefficient 0.3....	16
Figure 2.20 – IDS01 elastic model with pre-tension 6300 N, without friction	16
Figure 2.21 – IDS01 plasticity model with pre-tension 6300 N and friction coefficient 0.3 ..	17
Figure 2.22 – Flexibility comparison semi-empirical equations	19
Figure 3.1 – Shell model with fine mesh	21
Figure 3.2 – Example of deformed shell model.....	22
Figure 3.3 – Parameter: plate material	24
Figure 3.4 – Parameter: bolt material	25
Figure 3.5 – Parameter: plate thickness	25
Figure 3.6 – Parameter: bolt size	26
Figure 3.7 – Parameter: bolt spacing	26
Figure 3.8 – Parameter: plate width.....	27
Figure 3.9 – Definition of sections in 3-bolted models	28
Figure 3.10 – Load distribution for 3-bolted 3D model.....	28
Figure 3.11 – Load distribution for 3-bolted shell model.....	28
Figure 3.12 – Diameter function $k(d)$	29
Figure 3.13 – Thickness function $k(t)$	30
Figure 3.14 – Scale factor $k(d,t)$	31

Tables

Table 2.1 – Required pre-tension force specified from manufacturer (Huckcomp).....	8
Table 2.2 – Properties for specimens.....	10
Table 2.3 – Differences between experimental and benchmark 3D models.....	20
Table 3.1 – Parametric study matrix for benchmark 3D models	23
Table 3.2 – Flexibilities in mm/MN	23
Table 3.3 – Flexibilities per parameter in mm/MN	24
Table 3.4 – Constant scale factor of 1.5 for radius input (mm/MN)	29
Table 3.5 – Variable scale factor for radius input (mm/MN)	31
Table 3.6 – ABAQUS and NASTRAN shell model vs 3D model	32

Notation and units

Notation	Description	Unit
C	flexibility	mm/N
k	stiffness	N/mm
P	tensile force	N
δ	displacement	mm
d	diameter	mm
t	thickness	mm
E	Young's modulus	MPa
G	Shear modulus	MPa
I	Second moment of area	mm ⁴
k(d,t)	Equation for scale factor	-

1 Introduction

1.1 Objective

At stress analysis of aircraft structures it is important to have an accurate representation of the fastener flexibility. This is especially important at design of composite structure due to the brittle failure behaviour, i.e. no load redistribution between fasteners due to plastic deformation.

The objective of the work in this report is to find the best technique to represent the fastener flexibility at different modelling situations.

A second objective is to find a 3D modelling technique that makes it possible to virtually determine the fastener flexibility, i.e. exchange tests with FE.

A third objective is to examine the pre-processor Hyper Mesh and the ‘morphing’ technique, making it possible to change the geometry for the modelled fastener joint in a simple way and by that reduce modelling cost.

1.2 Background

Bolted joints remain as the most common bonding method in major structures. As a structural component, it is often considered the critical part of an assembly. However, research has not fully determined the effects of, i.e. geometric variability, material properties etc. As there are many ways of using Finite Element Analysis, FEA, it is very important to get an understanding of the different modelling techniques that may be used.

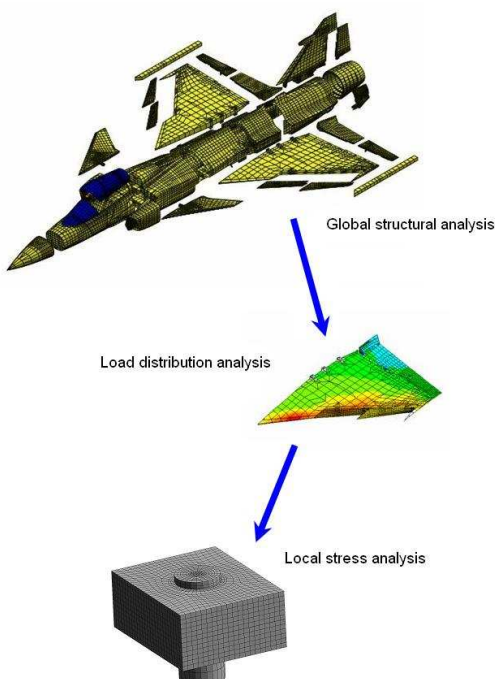


Figure 1.1 – Typical analysis and design procedure

As with most computational methods, FEA is highly dependent of computer processing time. It is desirable to cut time & costs by using simplified models, yet still get accurate and reliable results. The ability to use FEA early on in product development is most likely positive, if used correctly. For example, full 3D models are still not an option for global structures. Even in load distributional models it is uncommon to use a full 3D approach. Therefore, alternatives need to be evaluated, and in this case the turn has come to examine modelling of fastener flexibility in simplified 2D load distribution models.

A typical procedure for bolt design is shown in Figure 1.1. The global structural analysis is based on the performance specification of the object of interest. These are usually modelled with shells, to find a global load distribution. From here, parts of the global structure are examined further, with a more detailed analysis. These may be modelled with shells or a combination of shells and 3D brick elements. When the local load distribution is established, a detailed analysis of single parts may be performed using the data from previous steps in the procedure.

With the objective of this work in mind, briefly presented in Chapter 1.1, the procedure is somewhat reversed. Local flexibility analyses of detailed 3D models are verified with experiments, which in turn builds a benchmarking base for equivalent shell model analysis. See Chapter 1.3 for more details.

A decision needs to be made about what effects to include in the analysis to simulate reality. It is crucial to find the most important factors, but also to leave out negligible factors that only would consume analysis time with no gain in accuracy for the model. Modifications may also be made when creating benchmark models from the first simulation. It should be noted that this report is restricted to shear loaded fasteners.

In the industry there are several analytical and semi-empirical formulas to be used when estimating bolt flexibility in a lap-joint (Jarfall, 1983);(Huth, 1984);(Södergren & Lundahl, 1986);(Segerfröjd, 1995). Most of them are based on simple mechanical theory, with an added touch of numerical factors taken from independent experimental validation. At Saab, the Grumman and Huth formula may be the most common. This and several others are discussed in Chapter 2.3.

Recent work (Olert, 2004) found a one-dimensional model to use in load redistribution analysis where damage has occurred. The Grumman formula was given a positive remark for accuracy in flexibility prediction, but it was also found that this was not true for all configurations considered. This is evaluated further in Chapter 3.2. It was also pointed out that transferring a one dimensional method to a shell modelling method demands a more sophisticated connector element. Secondary bending was found to have an impact on load distribution, and should therefore be considered to have influence on modelling and measuring the bolt flexibility.

ESDU (Engineering Sciences Data Unit) have developed both an analytical and a numerical method used for analysing fastener connections, using a FORTRAN code, which also have been evaluated and compared (Austin, 2004). They are found to be equivalent, but not in accordance with the industry formulas mentioned earlier in this section without modification. None of these two methods are therefore considered in this work.

Influence of friction and calculation of the frictional force have been discussed (Segerfröjd, 1995). A number of factors are mentioned to be critical in this matter, i.e. the variation of contact pressure, effect of partial slip and non slip etc. A formula to calculate this variation is appended. This method is to be considered far more complex than the actual problem, and an alternative method is used in Chapter 2.2 to find an appropriate coefficient.

1.3 Procedure

The work is divided into two parts. After the collection of background information and current knowledge, the first main task is to find a correct 3D modelling technique that can replace typical experiments at determination of fastener flexibility, see Chapter 2. The modelling technique is compared and verified with experiments (Huth, 1983), and may then be used as a general benchmark for future work. Basic understanding is obtained by gradually adding factors and validating their contribution, meaning that an extensive amount of possible material and geometric effects are evaluated in this part of the work.

Part two consists of the evaluation of several different modelling techniques, see Chapter 3. A set of important parameters are pre-defined and 3D benchmark models are run. Results from the analysis of the shell models are tested and compared to these. Industry formulas are also used as a reference as well as giving input data in some cases. These modelling techniques are then validated as feasible or non-feasible methods for general use in load distribution analysis, see the Conclusions in Chapter 4.

2 Determination of bolt flexibility using detail FE

The objective in this chapter is to produce a method of predicting bolt flexibility using a FE-model to simulate experimental tests. Experimental tests made by Huth acts as a reference. A natural side-effect during the development of this model is a gained understanding of the effect of different parameters in the analysis for future extension of the work.

2.1 FE model

For pre-processing purposes, Hyper Mesh is used to generate input files for the ABAQUS/Standard solver. To post-process the output results, Hyper View is used. A morphing technique implemented in Hyper Mesh (HyperMesh 8.0sr1 User's Manual) is used to produce a large amount of models with a slight geometric variation later in the parametric study in Chapter 3.2. This feature in the pre-processor allows macron to be created in order to perform scaling of chosen parameters, e.g. the thickness, width, length, bolt and hole diameter etc.

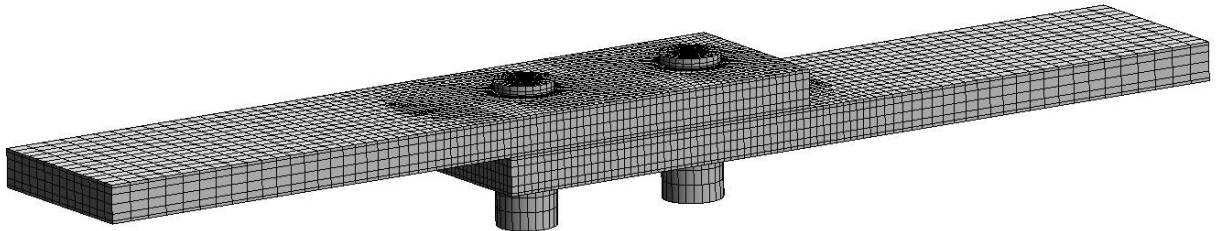


Figure 2.1 – Full view of 3D model

2.1.1 General definition

Brick elements are used to mesh the geometry of the detailed 3D models, with the ABAQUS Hex C3D8 element (ABAQUS 6.7-1 Keywords Reference), see Figure 2.1. The mesh density is made higher around areas of interest like bolt holes and plate surfaces, Figure 2.2. Through the thickness of the plates a mesh bias origin from the mid-plane is used to increase density close to the surface. This also had a positive effect on convergence of the contact iterations. Spring element SPRING2 is used to restrain rigid body motion of the bolts in the initial state. Boundary conditions are defined to simulate the reality of the experimental study (Huth, 1983), with both sides rigidly clamped except in the loading direction where the load is applied. Bolt rotation is also restrained around its axis through a dual clamping of both the top and bottom surfaces of each bolt. The load is applied as a prescribed displacement for one of the plate ends. In this way the singularities that usually appears is avoided.

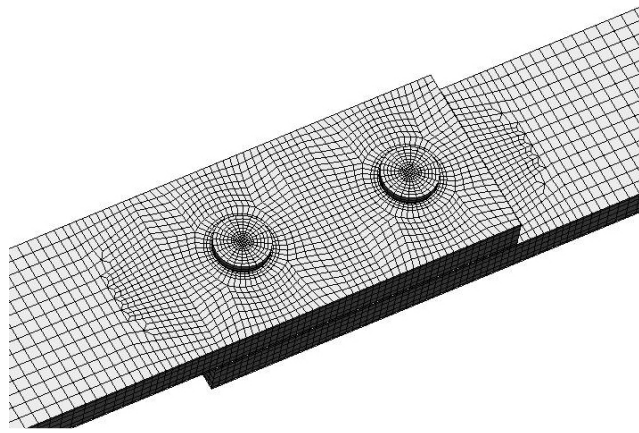


Figure 2.2 – Zoomed view of fine mesh

For models where pre-tension of bolts are used, three *STEP cards are put into the input file to define the loading sequence. The first card triggers the *PRE-TENSION card, which is used to define area and amount of the pre-tensional force. This force is fixed using the second *STEP card. The third and last card triggers the prescribed displacement mentioned earlier.

2.1.2 Defining contact

Contact is defined between bolts and plates as well as between the plates. The definition in Hyper Mesh is '3D element coated with shell'. Moreover, all contact surfaces use the 'surface to surface' formulation, as opposed to 'node to surface' where each node makes contact individually to the other surface. This may lead to discontinuity problems, i.e. some surfaces may not appear as smooth as they should when contact is made. Contact nodes are also adjusted prior to analysis, to associate the surfaces. The consequence of this is also a perfect bolt/hole fit in all models. Two different sliding approaches are also evaluated. The small sliding formulation assumes a limited amount of sliding for the nodal pairs which are associated initially. This has mostly a positive effect on processing time and the robustness of the model (convergence problems). Finite-sliding on the other hand lets the nodes slide 'freely', which may give a more accurate result compared to reality. It cannot be said though that the small sliding formulation converged better in all the different cases. The elements in contact need to be defined either as a 'master' or a 'slave' in each contact pair. This definition decides which element that could penetrate the other further if in contact, see Figure 2.3 for more details.

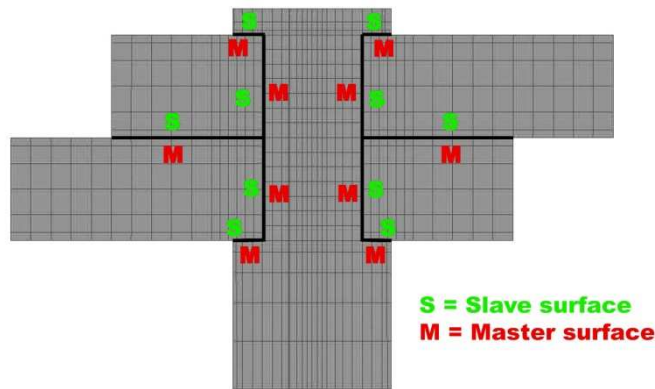


Figure 2.3 – Definition of master and slave surfaces

The Huth experiments (Huth, 1983) covered both protruded as well as countersunk bolt holes. His conclusion is that there are small differences in flexibility when comparing them, thus the focus of this report narrowed down to protruded heads only.

2.1.3 Defining friction

Static friction is defined with a single value. No other friction option is used, as friction data usually is relatively unknown. Various sources on the Internet (Beardmore, 2007); (Ramsdale, 2007) suggests values ranging from 0.3 to 1.35 for plate-to-plate friction for aluminium, depending on if the material has been anodized or if it has a treated surface of some kind. Hence, different values are evaluated and compared to experimental data in Chapter 2.2.

2.1.4 Defining material properties

Material data is taken from handbooks (MIL-HDBK-5E);(MMPDS-02). Plotted values for the aluminium Al 2024-T3 is shown in Figure 2.4, where the mean value of longitudinal and transverse is used, and titanium Ti 6Al4V in Figure 2.5 where the room temperature (RT) curve is used. These define plastic behaviour.

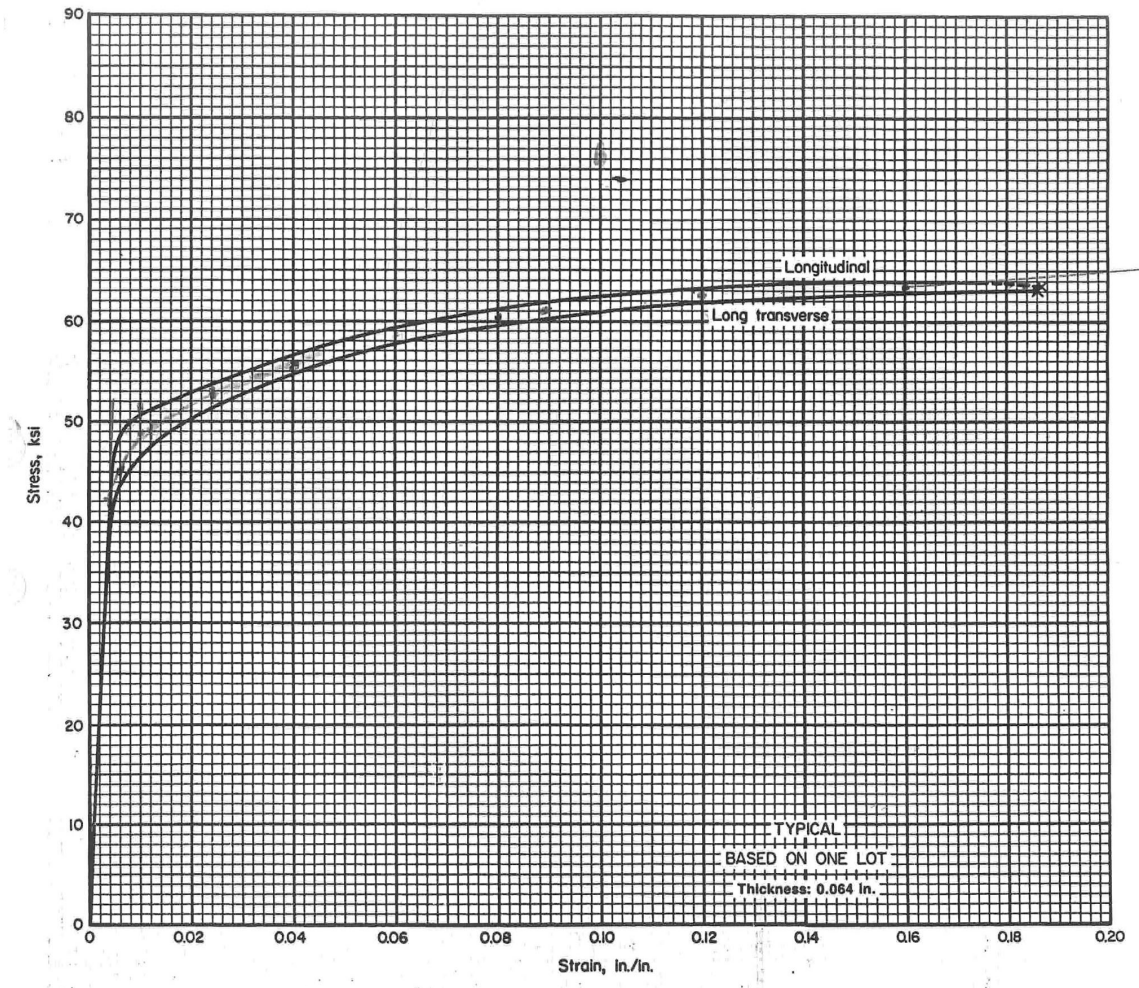


Figure 2.4 – Stress strain curve (full range) for Al 2024-T3 (MIL-HDBK-5E)

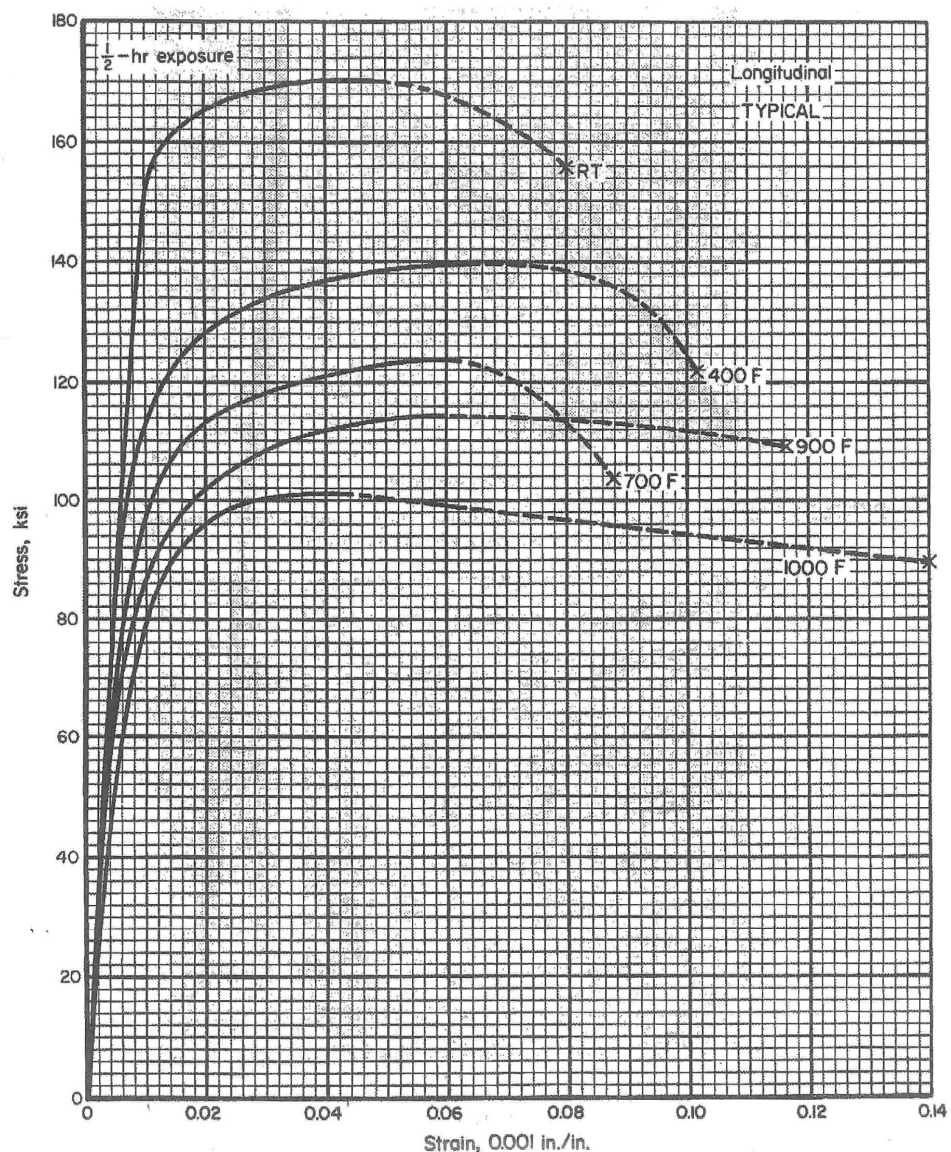


Figure 2.5 – Stress strain curve (full range) for Ti 6Al4V (MMPDS-02)

2.1.5 Using pre-tension

Pre-tension values are at first approximated to 6300 N for the 5 mm bolt diameter specimens. This corresponds well to the initial state of the bolt when it is tightened, which may be true for the simulation of the experimental studies. However, in the parametric study different values are used as the aim of this study is to simulate fastener pre-tension after several flights. Pre-tension force values also vary naturally with the size of the bolt. Information taken from the manufacturer (Huckcomp) is seen as a load decay chart in Figure 2.6 and in Table 2.1 as well.

SKIDMORE CLAMP LOAD DECAY HUCKCOMP, B, C / LGPL / HI-LITE / AND HI-LOK FASTENERS

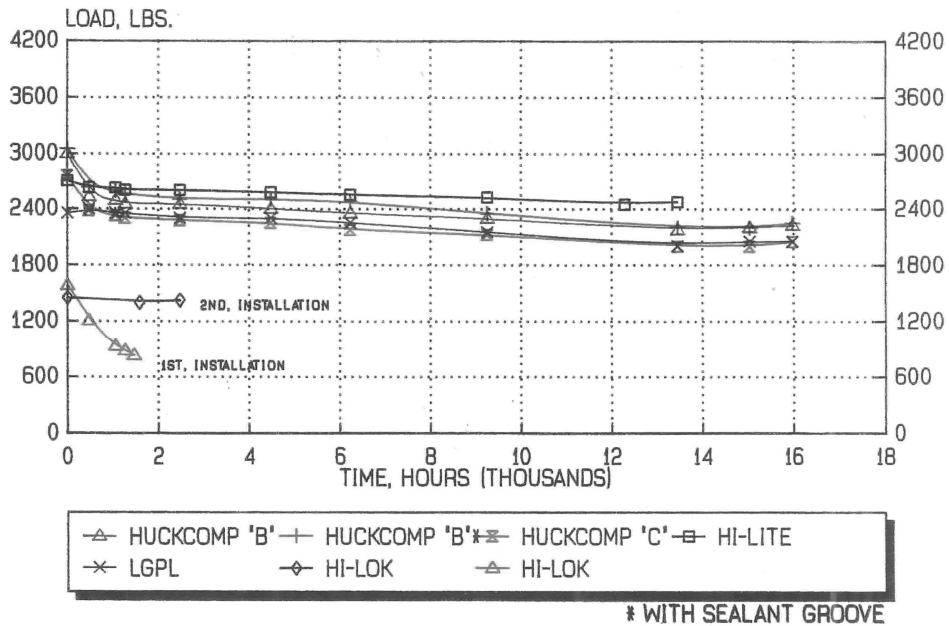


Figure 2.6 – Load decay for Hi-Lok fasteners (Huckcomp, 1991)

Pre-tension force, Lockbolt

Lockbolt material Ti 6Al4V

Collar material Pure Ti

Type	Beteckning	Collar	Diameter (inch)(mm)	Dia head (mm)	Height head (mm)	Preload measured (lbs)	measured (N)	requirement (lbs)	requirement (N)
130 csk head	LGPL9SC-V05B08	SLFC-MV05	5/32			1060	4715,092	700	3113,74
Prot. Head	HLGPL9SP-V05B06	SLFC-MV05	5/32 / 3.97	8,2	1,2	1014	4510,4748	700	3113,74
100 csk head	LGPL8SC-V06B10	SLFC-MV06	3/16			1446	6432,0972	800	3558,56
130 csk head	LGPL9SC-V06B10	SLFC-MV06	3/16			1394	6200,7908	800	3558,56
Prot. Head	HLGPL9SP-V06B10	SLFC-MV06	3/16 / 4.76	9,8	1,57	1414	6289,7548	800	3558,56
100 csk head	LGPL8SC-V08B06	SLFC-MV08	1/4			2315	10297,583	1500	6672,3
	LGPL8SC-V08B12	SLFC-MV08	1/4			2756	12259,2392	1500	6672,3
130 csk head	LGPL9SC-V08B11	SLFC-MV08	1/4			2443	10866,9526	1500	6672,3
Prot. Head	HLGPL9SP-V08B10	SLFC-MV08	1/4 / 6.35	12,4	1,93	2680	11921,176	1500	6672,3
130 csk head	LGPL9SC-V10B13	SLFC-MV10	5/16 / 7.93	15,5	2,18	4366	19420,8412	2500	11120,5

Table 2.1 – Required pre-tension force specified from manufacturer (Huckcomp)

2.2 Verification of 3D-model with experiments

An extensive experimental evaluation of fastener flexibility was made by Huth (1983). The 3D models mentioned in Chapter 2.1 are verified with three experiments from Huth: a single-shear with dual Hi-Lok bolts, a single-shear specimen with thinner plates and riveted aluminium joints and finally a double-shear specimen with a single Hi-Lok bolt. All fasteners have protruding heads. From the report of the experimental studies (Huth, 1983), these are labelled ISS11 (Figure 2.1), IISS06 (Figure 2.7) and IDS01 (Figure 2.8) respectively. For a full list of details, see Table 2.2.

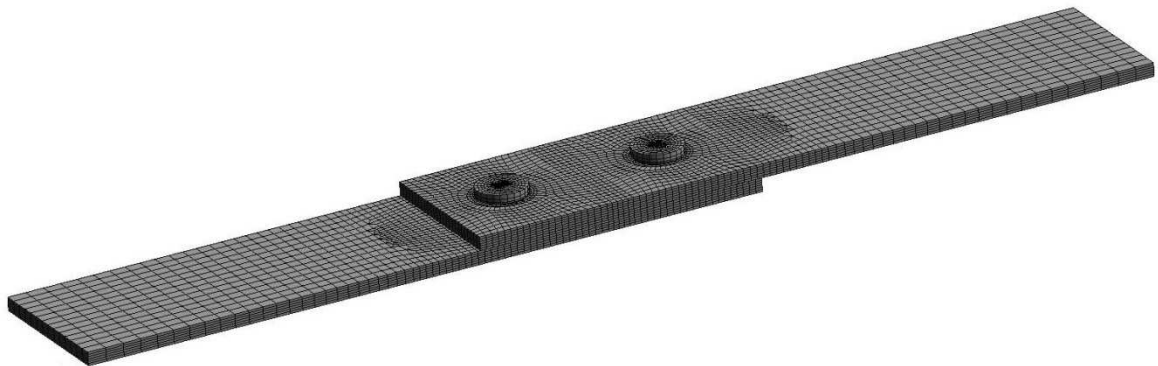


Figure 2.7 – Specimen IISS06

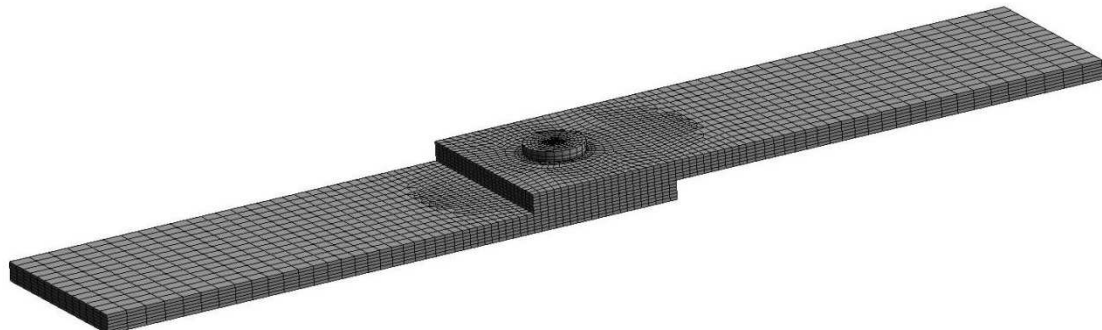


Figure 2.8 – Specimen IDS01

In Figure 2.8, note how symmetry is used to reduce processing time. The middle plate in the model is split in half and translation in the transverse direction is constrained.

2.2.1 Measurement definition of specimens

The FE results need to be measured in a similar way as the original experiments, where a 50 mm extensometer was attached to each specimen, measuring over both fasteners. This meant a two-point magnitude measurement system has to be used for the model as well (Figure 2.11), to extract the proper values and effect of secondary bending. Dimensions for the plates are defined in Figure 2.9 and Figure 2.10.

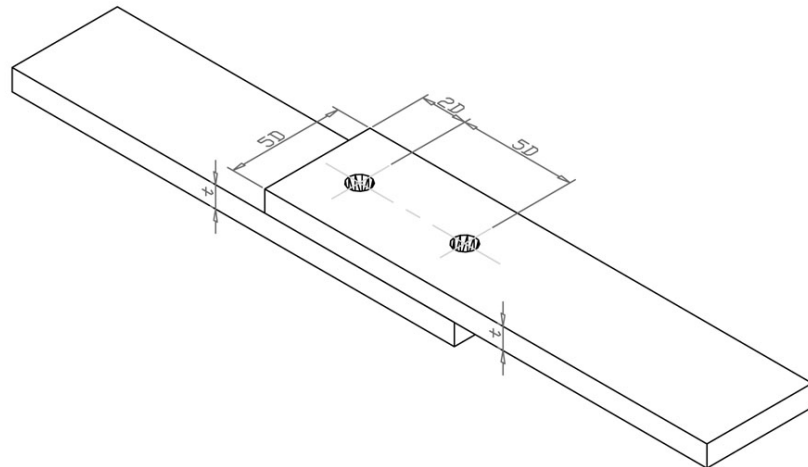


Figure 2.9 – Geometry definition for single shear joints

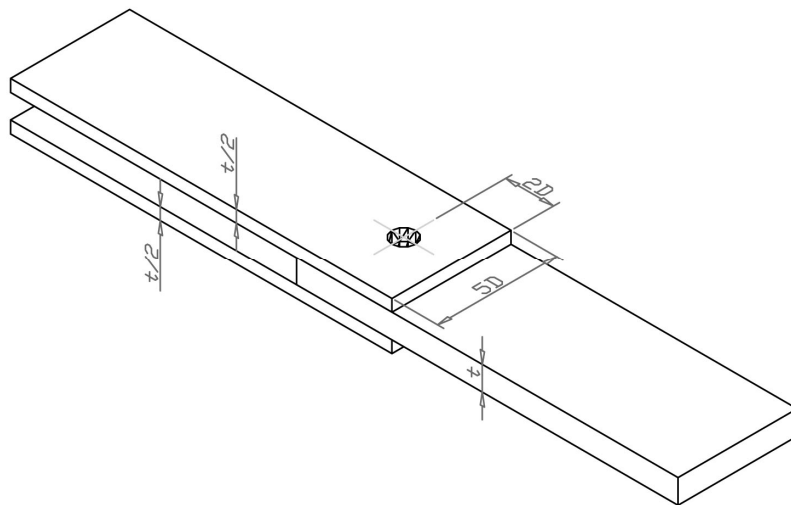


Figure 2.10 – Geometry definition for double-shear joints

Specimen	Fastener diameter	Fastener type	Thickness	Width	Plate material	Fastener material	Type of joint
ISS11	5 mm	Hi-Lok	5.1 mm	25 mm	Al 2024-T3	Ti 6Al4V	Single
ISS06	4.8 mm	Rivet	2.0 mm	24 mm	Al 2024-T3	Al 2024-T3	Single
IDS01	5 mm	Hi-Lok	5.1 mm	25 mm	Al 2024-T3	Ti 6Al4V	Double

Table 2.2 – Properties for specimens

From here, the fastener flexibility is calculated, see equations below. In the dual bolt case, it is assumed that the load is evenly distributed between the two fasteners. Note

the general measurements points in Figure 2.11 and Figure 2.12. Calculations are taken from Huth (1983):

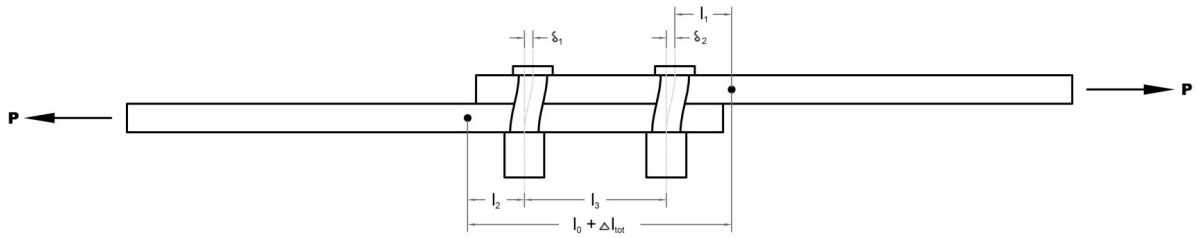


Figure 2.11 – Measurement definition for single-shear lap-joint

$$\Delta l_{tot} = \frac{\delta_1 + \delta_2}{2} + \Delta l_1 + \Delta l_2 + \Delta l_3 \quad \text{Eq. 2.1}$$

$$\delta = \frac{\delta_1 + \delta_2}{2} = \Delta l_{tot} - \Delta l_{elast} \quad \text{Eq. 2.2}$$

$$\Delta l_{elast} = \frac{P}{t_1 w E_1} \left(l_1 + \frac{l_2}{t_2 \cdot \frac{E_2}{E_1}} + \frac{l_3}{1 + \frac{t_2}{t_1} \cdot \frac{E_2}{E_1}} \right) \quad \text{Eq. 2.3}$$

$$\begin{cases} C_1 = \frac{\delta_1}{P/2} \\ C_2 = \frac{\delta_2}{P/2} \end{cases} \quad C_1 + C_2 = \frac{\delta_1 + \delta_2}{P/2} \quad \text{Eq. 2.4}$$

$$C = \frac{1}{2}(C_1 + C_2) = \frac{1}{2} \cdot \frac{\delta_1 + \delta_2}{P/2} = \frac{\delta_1 + \delta_2}{P} \quad \text{Eq. 2.5}$$

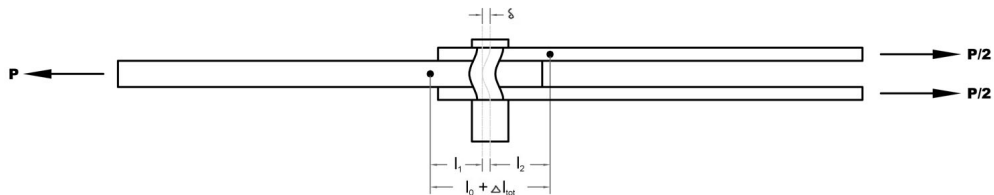


Figure 2.12 – Measurement definition for double-shear lap-joint

$$\Delta l_{tot} = \delta + \Delta l_1 + \Delta l_2 \quad \text{Eq. 2.6}$$

$$\delta = \Delta l_{tot} - (\Delta l_1 + \Delta l_2) = \Delta l_{tot} - \Delta l_{elast} \quad \text{Eq. 2.7}$$

$$\Delta l_{elast} = \frac{P}{w} \left(\frac{l_1}{t_1 E_1} + \frac{l_2}{2t_2 E_2} \right) \quad \text{Eq. 2.8}$$

$$C = \frac{\delta}{P} \quad \text{Eq. 2.9}$$

The accuracy of the model depends on several factors such as material property definition, friction, contact type formulation and pre-tension. Step by step, each of the factors is included in the analysis. This study makes it possible to determine the specific effect from each of them. Specimen ISS11 is used as a main reference.

2.2.2 Results

Firstly, material properties are investigated. The first runs of the reference model contains only elastic material data, resulting in the near linear behaviour seen in Figure 2.14. When adding plastic material data from Figure 2.4 and Figure 2.5, the response becomes non-linear. From here, pre-tension is added (Huckcomp), the measured values in Table 2.1. A set of tests determining the effect of pre-tension is seen in Figure 2.15. This also improves convergence time for the model, as a positive side-effect. Lastly, friction coefficients are defined. This is the single most unknown figure in the analysis. As discussed in Chapter 2.1.3, values ranging between 0.3 and 1.35 were recorded for these particular materials. Also mentioned in Chapter 0, an analytical method is present (Segerfröjd, 1995). As this formula is based on varying pressure across the contact area, it gives the force acting on the plates, not the actual friction coefficient.

Frictional force (Segerfröjd, 1995):

$$F(x) = 2\pi mn \int_x^{x_0} x \mu_x p_x dx \quad \text{Eq. 2.10}$$

Thus, the only reasonable solution is to test a range of different static coefficients, see Figure 2.16. The final result for specimen ISS11 is shown in Figure 2.17 plotted with the experimental result. A general deformed shape is seen in Figure 2.13. Results for IISS06 and IDS01 are shown in Figure 2.18 and Figure 2.19 as well as in Figure 2.20 and Figure 2.21, respectively.

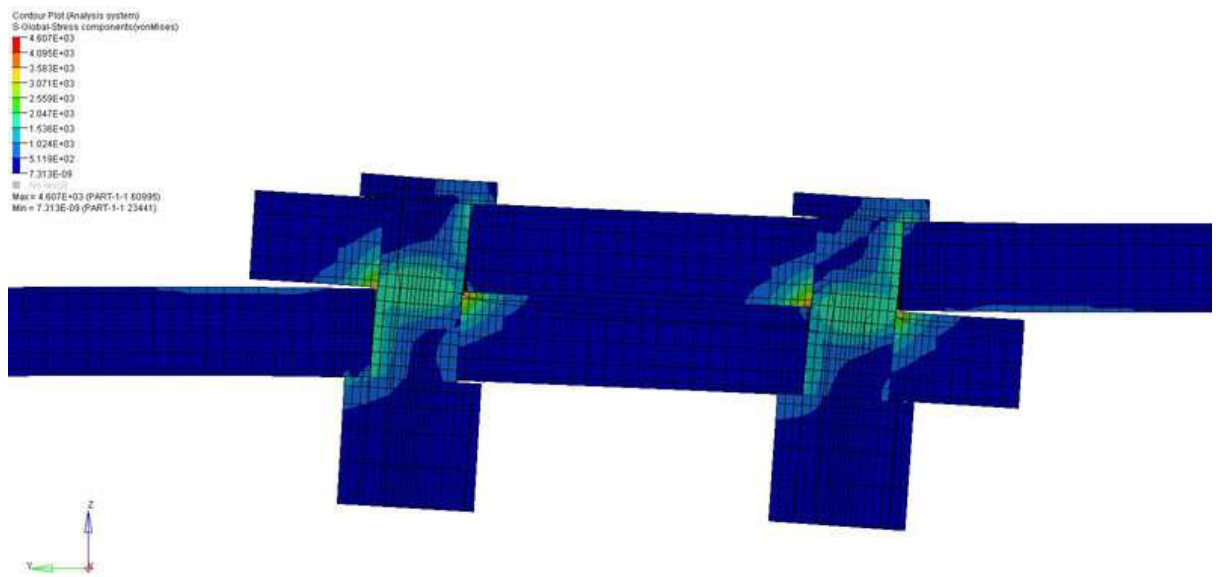


Figure 2.13 – Zoomed section of elastic ISS11 specimen

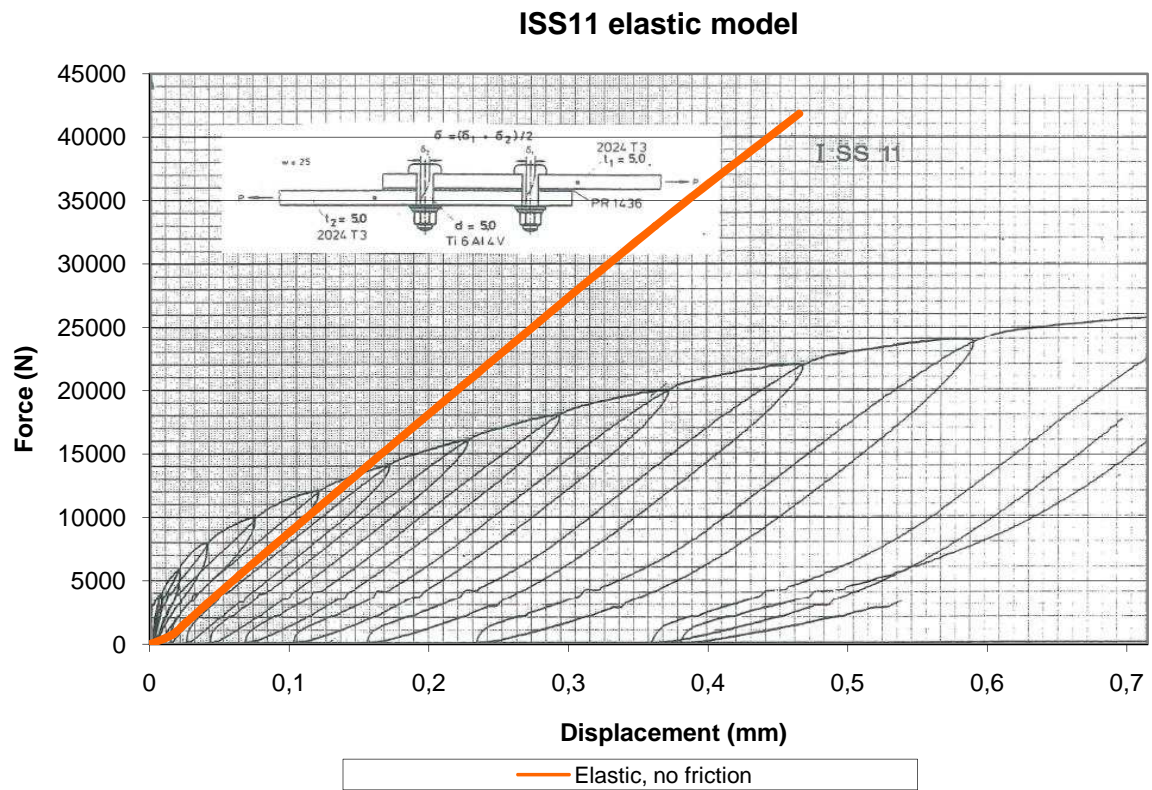


Figure 2.14 – Elastic model with pre-tension 6300 N, without friction

ISS11 comparison chart, different pre-tensions

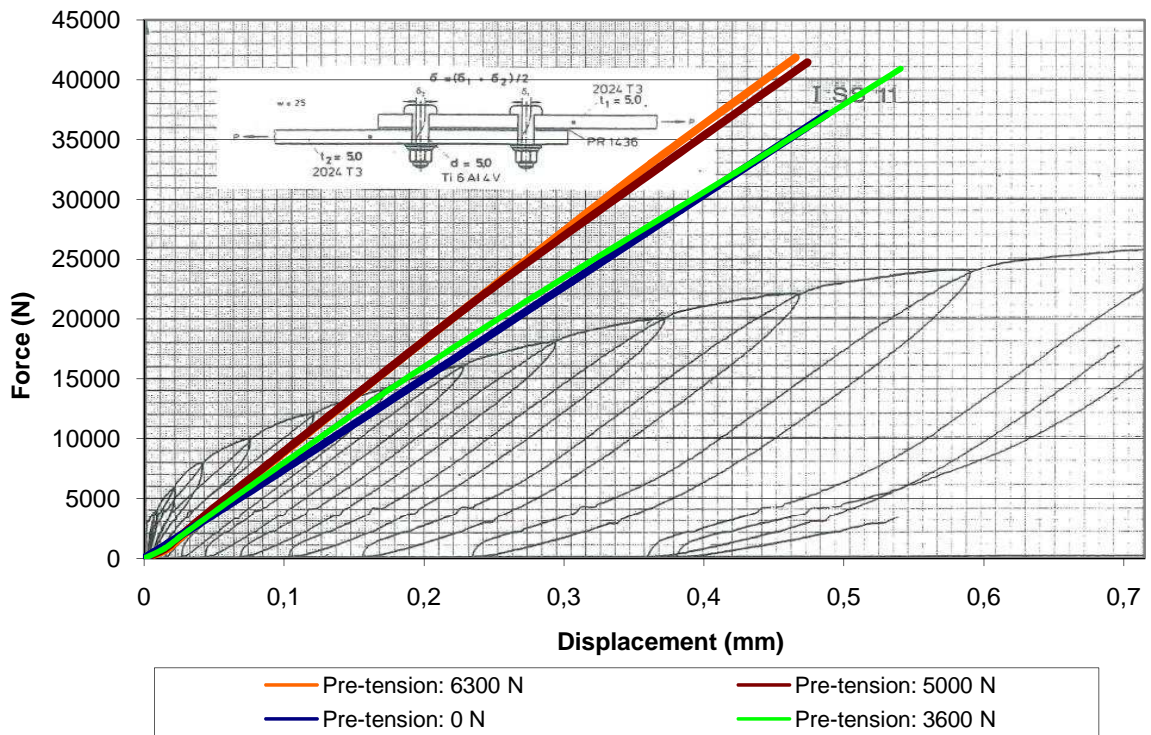


Figure 2.15 – Effect of pre-tension parameter, no friction used

ISS11 comparison chart, different friction coefficients

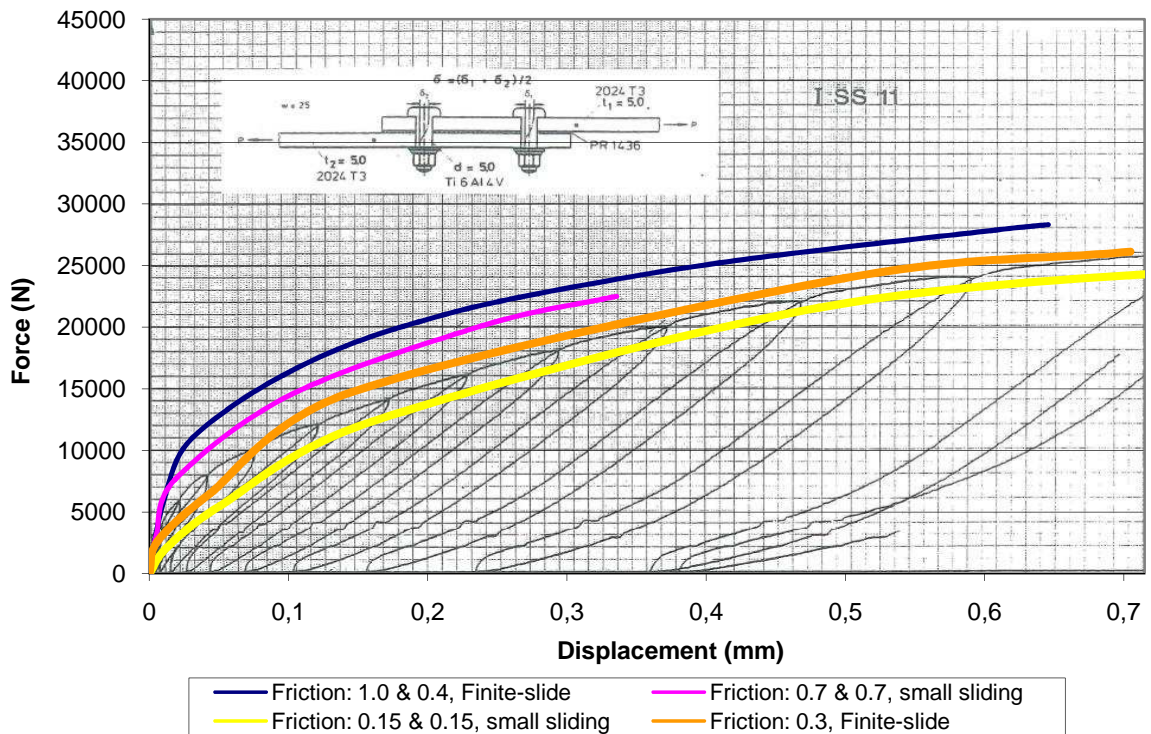


Figure 2.16 – Effect of friction parameter, with plasticity and pre-tension 6300 N

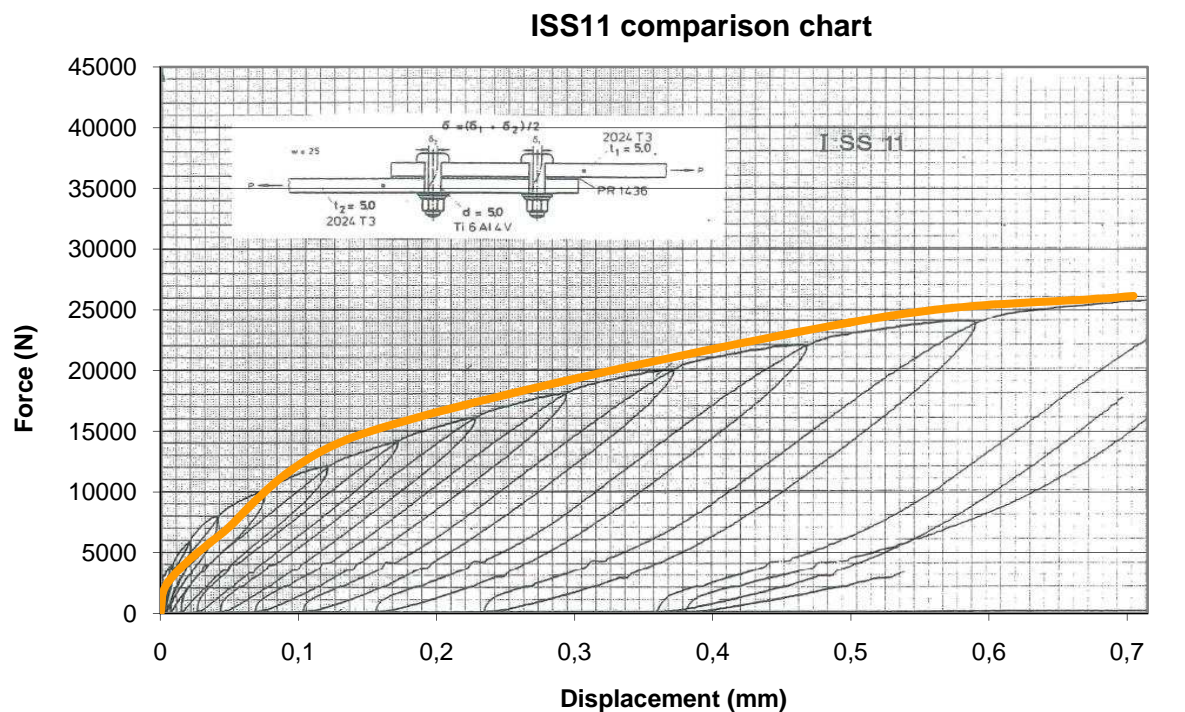


Figure 2.17 – ISS11 plasticity model with pre-tension 6300 N and friction coefficient 0.3

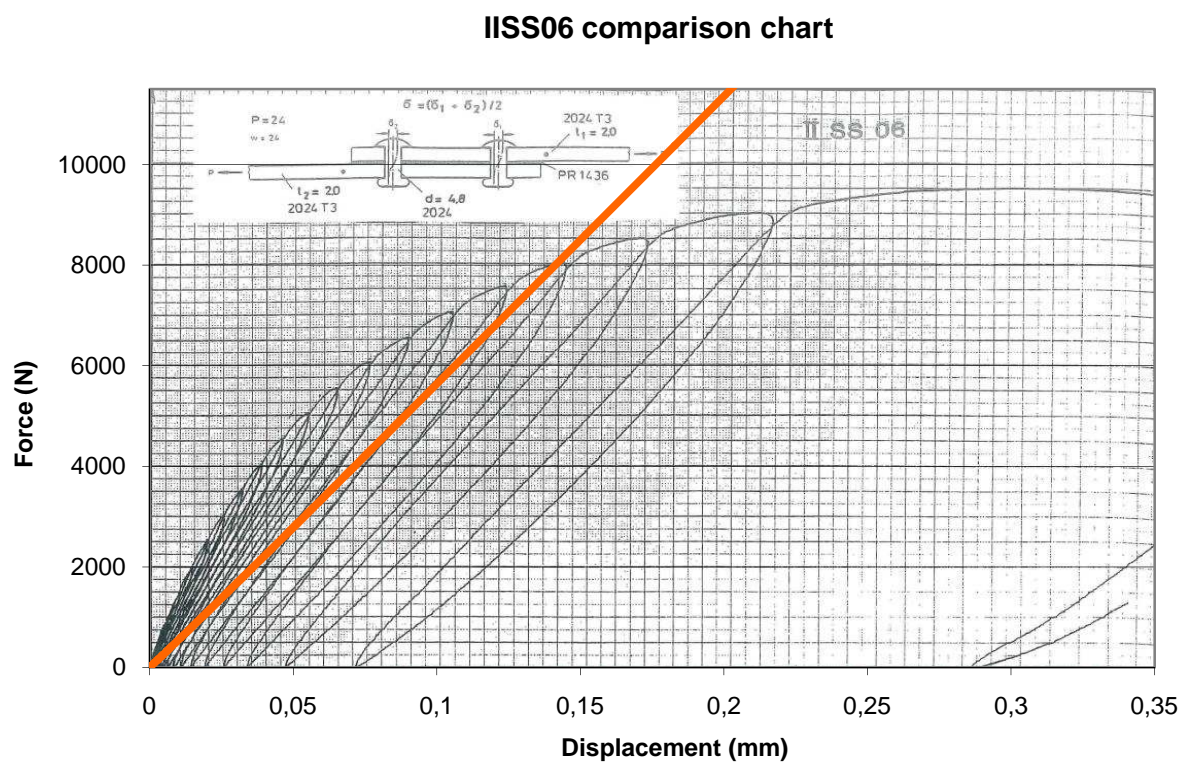


Figure 2.18 – IISI06 elastic model with pre-tension 500 N, without friction

IIS06 comparison chart

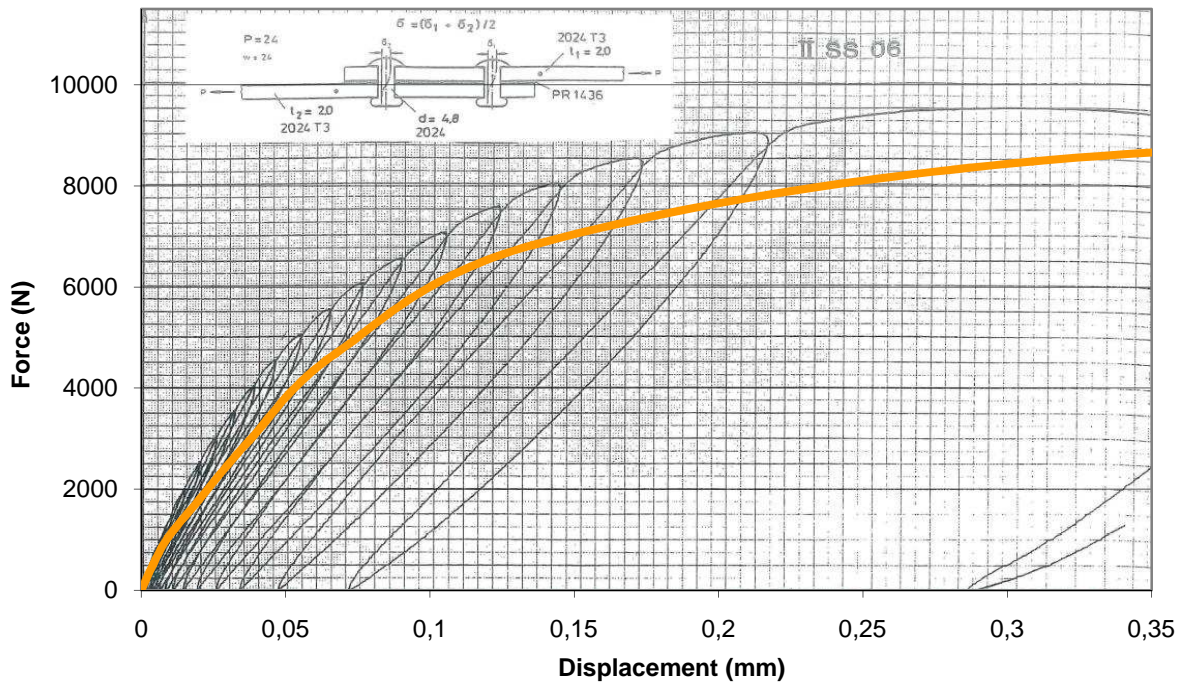


Figure 2.19 – IIS06 plasticity model with pre-tension 500 N and friction coefficient 0.3

IDS01 comparison chart

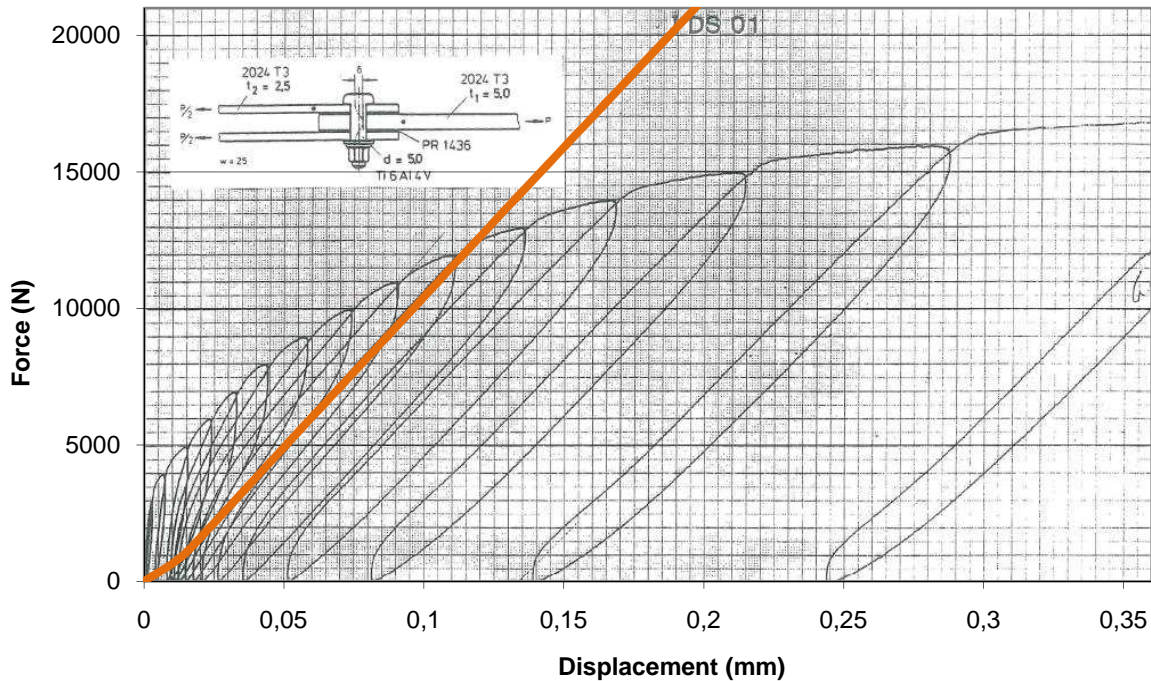


Figure 2.20 – IDS01 elastic model with pre-tension 6300 N, without friction

IDS01 comparison chart

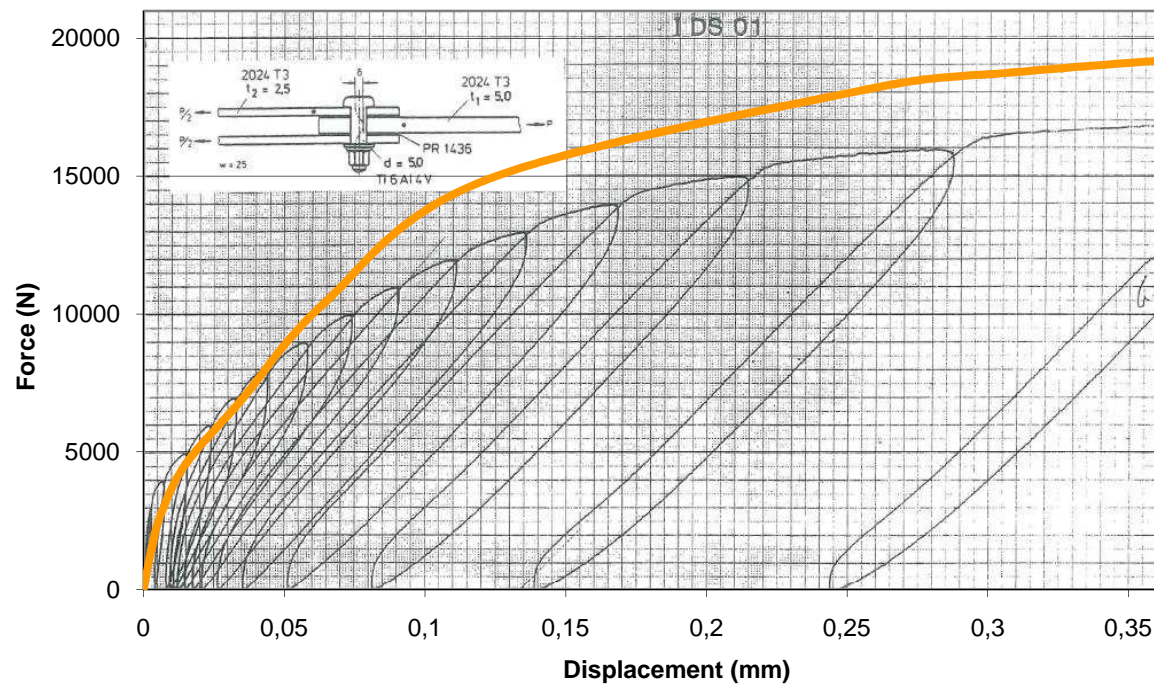


Figure 2.21 – IDS01 plasticity model with pre-tension 6300 N and friction coefficient 0.3

2.3 Comparison with empirical equations

There are several known semi-empirical equations suitable for the prediction of fastener flexibility. Previous work include methods developed and used by Huth (Huth, 1984), Grumman (Jarfall, 1983), Boeing (Jarfall, 1983), Douglas (Jarfall, 1983) to mention a few. Looking at Figure 2.22 it is clear that these equations predict bolt flexibility with a wide variation of result. This variation may be due to neglected geometric and physical features normally found on fasteners, such as pre-tension, bolt spacing, surface roughness, use of primer or sealant etc. In some cases secondary bending, which is applicable for single shear fasteners, is accounted for with empirical factors, in other cases not. This may however be crucial in further analysis to get accurate results.

Huth equation:

$$C = \left(\frac{t_1 + t_2}{2d} \right)^a \cdot \frac{b}{n} \left(\frac{1}{t_1 E_1} + \frac{1}{nt_2 E_2} + \frac{1}{2t_1 E_1} + \frac{1}{2nt_2 E_2} \right) \quad \text{Eq. 2.11}$$

where

$a=2/3$ and $b=3$ for protruded metallic bolts

$n=1$ for single-shear lap-joints and $n=2$ for double-shear lap-joints

Grumman equation:

$$C = \frac{(t_1 + t_2)^2}{E_b d^3} + 3,72 \left(\frac{1}{t_1 E_1} + \frac{1}{t_2 E_2} \right) \quad \text{Eq. 2.12}$$

Boeing's two equations:

$$C = \frac{4(t_1 + t_2)}{5G_b A_b} + \frac{t_1^3 + 5t_1^2 t_2 + 5t_1 t_2^2 + t_2^3}{40E_b l_b} + \frac{t_1 + t_2}{t_1 t_2 E_b} + \frac{1}{t_1 E_1} + \frac{1}{t_2 E_2} \quad \text{Eq. 2.13}$$

$$C = \frac{2^{(t_1/d)^{0.85}}}{t_1} \left(\frac{1}{E_1} + \frac{3}{8E_3} \right) + \frac{2^{(t_2/d)^{0.85}}}{t_2} \left(\frac{1}{E_2} + \frac{3}{8E_3} \right) \quad \text{Eq. 2.14}$$

Douglas equation:

$$C = \frac{1}{Ed} \left(A + Bd \left(\frac{1}{t_1} + \frac{1}{t_2} \right) \right) \quad \text{Eq. 2.15}$$

where

$A=5$ for aluminium rivet and $A=1,67$ for steel bolts

$B=0,80$ for aluminium rivet and $B=0,86$ for steel bolts

It may be seen on the character of the equation whether it supports secondary bending adjustment or if the effect is neglected. As an example, the Huth equation does not differentiate between single- and double-shear lap-joints in this case. This fact makes it easy to assume that secondary bending is not taken into account for the single-shear lap-joint, as the double-shear lacks the effect per definition. On the contrary, the Grumman formula is based on an empirical factor in the second term of the equation, to adjust for secondary bending. This also leads to a limitation as it cannot be used for double-shear lap-joints. Boeing's equation no. 1 is taking secondary bending into account with an analytical solution, the second equation though is from an unknown source and thus, it cannot be said for certainty. The same applies to the Douglas equation.

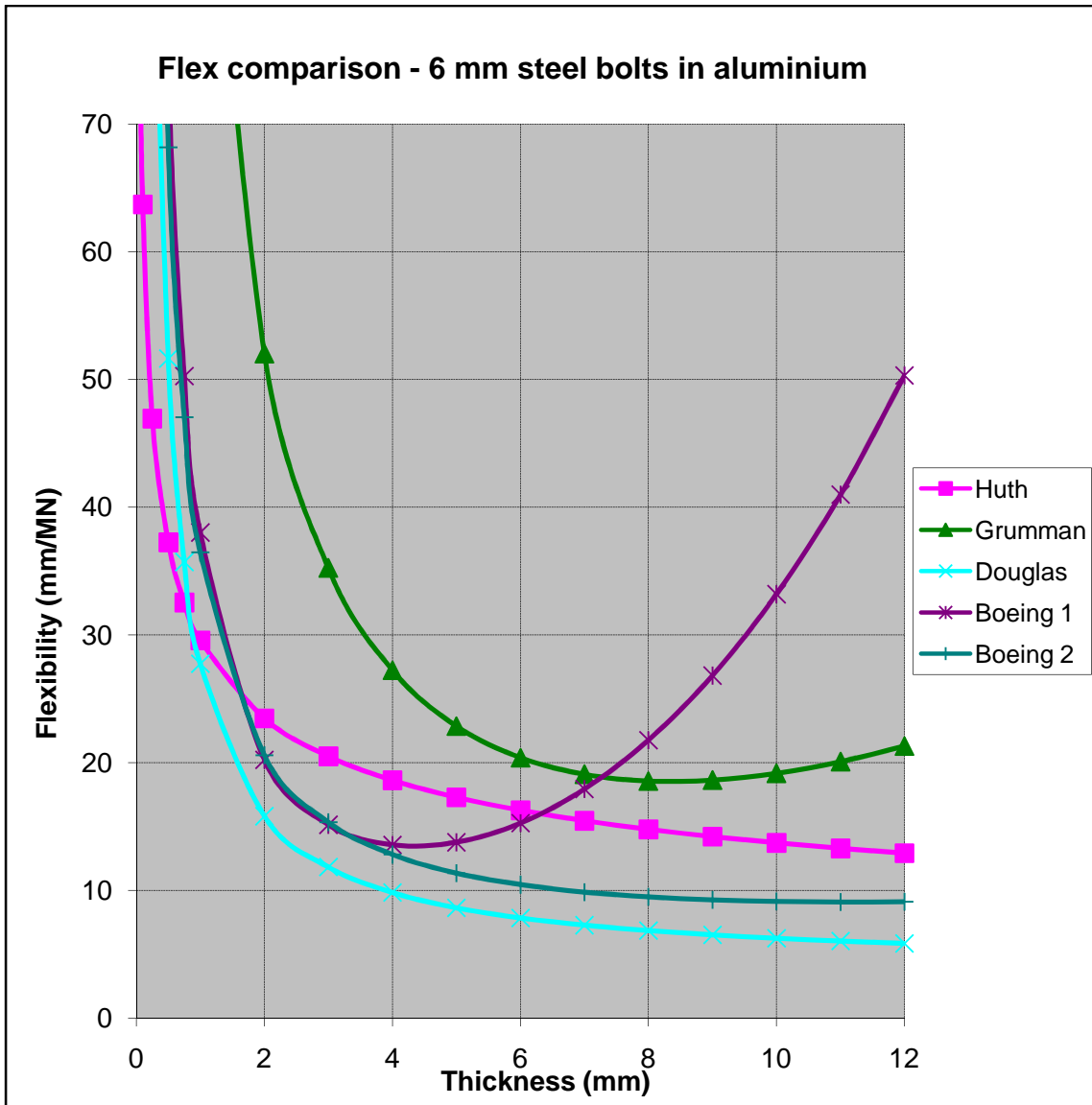


Figure 2.22 – Flexibility comparison semi-empirical equations

2.4 Conclusions

Looking at Figure 2.17, Figure 2.19 and Figure 2.21 it is fair to say that there is a relatively good correlation between FE and experiments regarding flexibility. Plasticity seems to be the most significant factor in order to achieve good correlation with the experimental results. This is most likely the result of stress concentrations in combination with plasticity around the holes and the bolts where contact is made, and where plasticity occurs earlier than for the rest of the model. Other factors, like the different friction coefficients used and the amount of pre-tension, has more of a fine tuning characteristic during analysis. This model may also be an option to traditional experimental work in general, as this simulation is accurate enough in terms of predicting fastener flexibility.

The elastic limit is extended for each hysteresis loop, giving a more linear behaviour for the fastener flexibility. This fact leads to a reason to believe that plasticity data for both the bolt and plates may be removed at determination of flexibility for use in load distribution models. The elastic curve corresponds well with the elastic regions of the experimental charts in Figure 2.14, especially after several of the quasi-static loops are made. This concludes that at the design point of the fastener, plastic deformation has extended the linear relation between displacement and applied force enough to be removed. Fasteners are generally considered to weaken when used and its original strength and flexibility is degraded, so this assumption is logical.

Further simplification may however be needed to come closer to the “true” load case of the forthcoming load distribution model. If the model is supposed to be accurate for the several flights case, a slight modification needs to be done for the pre-tension and friction values as well. Friction is set to zero, to let the load be transferred by the bolts only. Pre-tension is naturally relaxed as time goes by, and with the aid of Figure 2.6 and Table 2.1 in Chapter 2.1, a minimum requirement may be used for each bolt dimension used for the benchmark models. A summary of the differences is listed in Table 2.3, for the ISS11 single-shear specimen.

Parameter	Experimental 3D model	Benchmark 3D model
Pre-tension	6300 N	3600 N
Friction coefficient	0.3	0.0
Plasticity	Yes	No

Table 2.3 – Differences between experimental and benchmark 3D models

3 Modelling technique - Load distribution models

There are several possible ways of modelling fastener flexibility together with shell elements for the plates. The first option is to find an element representing the bolt with input solely relying on material and geometric data. A second option is to calculate the flexibility from either of the semi-empirical equations mentioned in Chapter 2.3 or from an equivalent 3D model. This flexibility is then possible to use with spring elements attached to the plates. Both options are considered and evaluated in this chapter, and are referred to as beam element method and connector element method, respectively.

3.1 FE model

The general model is built up by ABAQUS four-node shell elements (ABAQUS 6.7-1 Keywords Reference), Figure 3.1. At the bolt centre points, nodes are connected with connector or beam elements. Boundary conditions are fully clamped at both ends to simulate the clamping mechanism in the experimental tests and the 3D model. This means all translations are set to zero at the left end, along with rotation in the transverse direction. One of the nodes is also clamped in the remaining two degrees of freedom. The other end is clamped similarly, except for the translation in the loading direction.

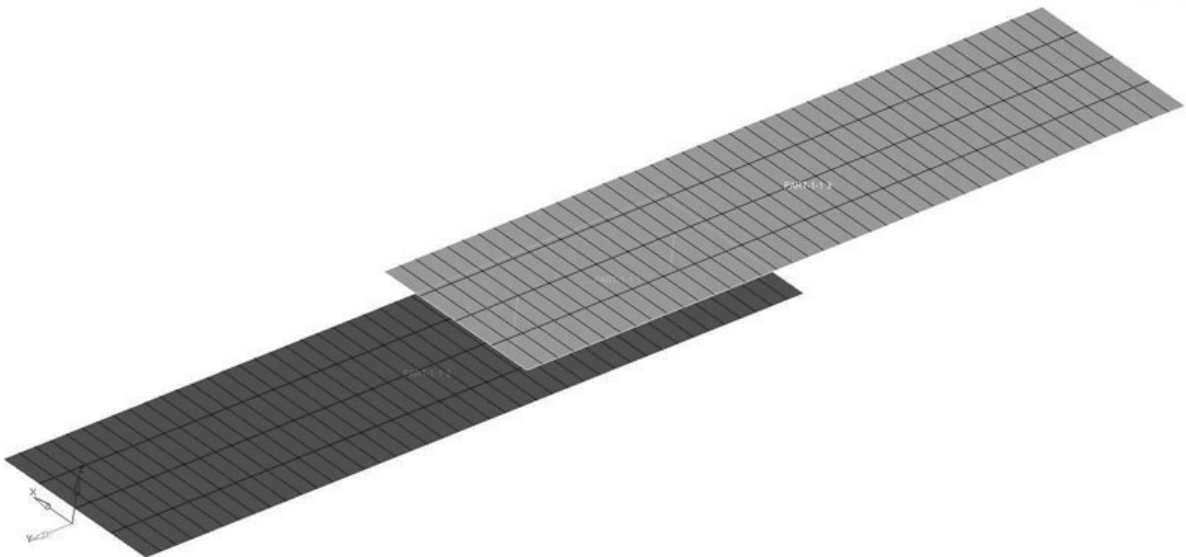


Figure 3.1 – Shell model with fine mesh

Only linear elastic material properties are used for these models, as they are to be compared with the benchmark 3D models, see Chapter 2.4. Two different mesh densities are evaluated. The shell model with fine mesh density is seen in Figure 3.1. An alternative model is also produced with a more coarse mesh in the loading direction for investigation of this parameter. The mesh density in the width direction is not modified. Models with beam elements connecting the plates are loaded with a prescribed displacement similar to the detailed 3D models in Chapter 2. For the connector element connected models a force is applied evenly to one of the ends with a multi-point constrain, as a prescribed displacement had convergence issues for this type of model. A general deformed shape is seen in Figure 3.2.

3.1.1 Beam Element Method

Input for the beam element consists of only the dimension given as a radius and the Young's modulus for the bolt material. The chosen sections of the beam elements are circular and only two-node beams (BAR2) have been used in the analyses. A natural offset is used of one plate thickness, which means that this method has inherent secondary bending when loaded in tension.

3.1.2 Connector Element Method

These connector elements are an assembled group of spring elements. Spring elements usually have only one degree of freedom, but combined together they may form a single connector element of either three or six DOF's (degrees of freedom) defined in ABAQUS (ABAQUS 6.7-1 Keywords Reference). These are three translational and three rotational DOF's. In this study only Cartesian connector elements are used, which only use the three translational DOF's. This means that the inverted flexibility, spring stiffness, needs to be defined in these directions. The stiffness needs to be calculated prior to analysis, which adds a step in the procedure. There are several methods of calculating these, as seen in Chapter 2.3. Care should be taken, as mentioned in the same chapter, whether offset is used or not. If it is used, it should be defined in the same way as for the Beam Element Method in Chapter 3.1.1. If the no offset option is used, the plates should be placed in the mean surface if possible. Some solvers may experience problems with infinitesimal lengths for elements, more on this in Chapter 3.4.

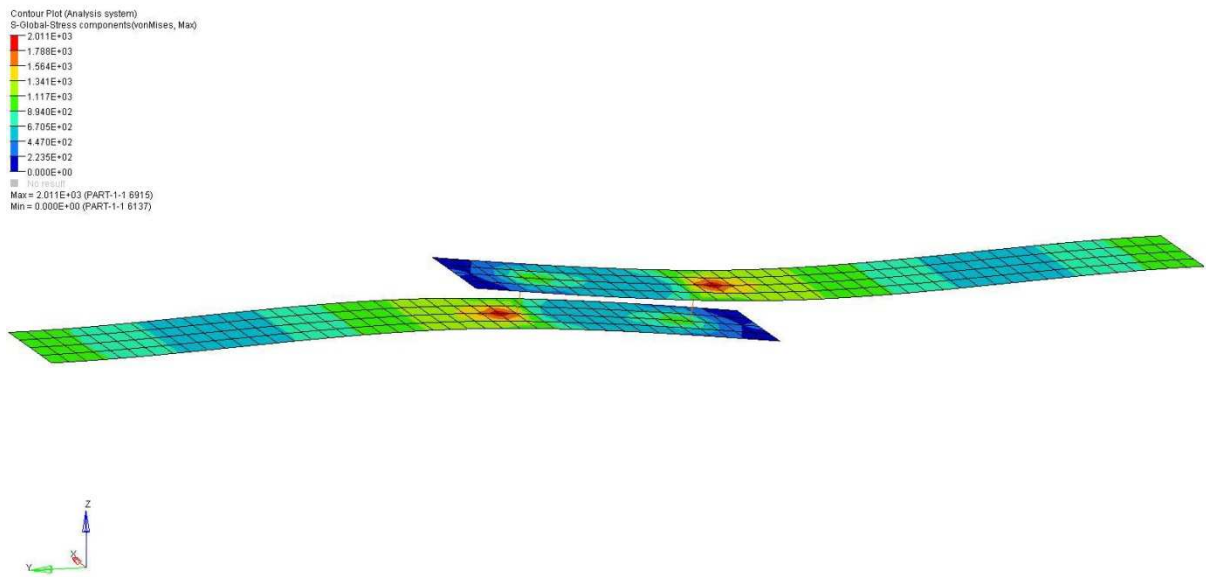


Figure 3.2 – Example of deformed shell model

3.2 Parametric study

Using shell elements, three different model parameters were evaluated. These were the use of beam versus connector elements representing the fastener, mesh density and offset based on plate thickness against no offset. This sum up to six different possible models with shells. These models were applied to a series of tests, where different aspects of bolt and plate geometry are varied. Each of these shell models has a

benchmark model, based on the 3D study in Chapter 2. The properties of the detailed 3D benchmark models are presented as a matrix in Table 3.1. The recommendations presented in Chapter 2.4 are used in these 3D analyses, i.e. no plasticity, no friction and a pre-tension equal with a minimum requirement. Flexibility results for the 3D benchmark models are presented in Table 3.2.

ANALYSIS	Bolt Diameter	Bolt E (MPa)	Plate t (mm)	Plate E (MPa)	spacing	Plate width	single/double	no of bolts	pre-tension (N)
1 (reference)	5	110300	5,1	72000	5D	5D	s	2	6300
2	5	110300	5,1	72000	5D	5D	s	2	3600
3	5	110300	5,1	50000	5D	5D	s	2	3600
4	5	110300	2,5	72000	5D	5D	s	2	3600
5	5	110300	7,5	72000	5D	5D	s	2	3600
6	4	110300	5,1	72000	5D	5D	s	2	3200
7	7,93	110300	5,1	72000	5D	5D	s	2	11200
8	5	110300	5,1	72000	5D	5D	d	2	3600
9	5	110300	5,1	72000	8D	5D	s	2	3600
10	5	110300	5,1	72000	5D	10D	s	2	3600
11	5	110300	5,1	72000	5D	5D	d	1	6300
12	5	110300	5,1	72000	5D	5D	s	1	3600
13	5	110300	5,1	72000	5D	5D	s	3	3600
14	7,93	110300	7,5	72000	5D	5D	s	2	11200
15	5	72000	5,1	72000	5D	5D	s	2	3600
16	4,8	72000	2	72000	5D	5D	s	2	500
17	5	210000	5,1	72000	5D	5D	s	2	3600
18	6,35	110300	5,1	72000	5D	5D	s	2	6700
19	6,35	110300	7,5	72000	5D	5D	s	2	6700

Table 3.1 – Parametric study matrix for benchmark 3D models

All used pre-tension values are minimum requirements; see Table 2.1 in Chapter 2.1.5, except 6300 N and 500 N which are estimated nominal values. Analysis number 16 represents a riveted joint while the other are bolted with Hi-Lok or Lockbolt. The different shell models with geometric data equivalent to the 3D benchmark models are shown in Table 3.2. This table is not complete as some of the analyses were not possible to perform, due to convergence issues for these models. Some configurations were also not interesting because of shortcomings in the model as such. The analyses were done working from top to bottom and when the accuracy of each configuration had been validated, only the foremost models were carried through.

3.2.1 Results

Each shell model analyses should be compared to its corresponding 3D analysis. This gives a secondary comparison where the different shell models are put against each other. Charts are presented per parameter in Figure 3.3 to Figure 3.8. These also have calculated values from the theoretical and semi-empirical equations in comparison.

ANALYSIS	Huth equation	Grumman equation	3D benchmark flexibility	connector offset small elem	connector no offset small elem	connector offset large elem	connector no offset large elem	beam offset small elem	beam offset large elem
2	21,96	27,81	30,34	66,62	33,45	63,66	33,30	34,84	33,24
3	29,25	36,72	34,82	86,56	39,28	82,32	39,04	45,68	43,31
4	27,85	43,15	45,78	112,54	52,14	101,02	51,90	49,73	46,15
5	19,31	30,10	29,17	43,38	31,29	42,38	31,18	36,51	35,45
6	25,48	35,00	36,82	75,58	39,97	72,62	39,82	43,46	41,89
7	16,15	22,15	-	-	-	-	-	26,55	24,97
8	10,98	-	14,48	-	-	-	-	8,50	8,34
9	21,96	27,81	28,00	-	33,45	-	33,33	32,06	30,50
10	21,96	27,81	26,68	-	31,56	-	31,46	29,05	27,82
11	10,98	-	9,87	-	-	-	-	8,56	8,51
12	21,96	27,81	-	-	-	-	-	27,82	26,59
13	21,96	27,81	31,67	-	-	-	-	34,95	33,36
14	14,20	17,87	-	-	-	-	-	22,25	33,17
15	24,84	31,82	33,36	-	36,46	-	36,32	40,10	38,66
16	34,87	53,68	44,29	-	52,24	-	51,92	61,06	57,16
17	19,40	24,22	25,61	-	28,71	-	28,56	29,97	28,47
18	18,73	23,95	24,26	-	-	-	-	29,50	-
19	16,47	21,74	24,24	-	-	-	-	27,14	-

Table 3.2 – Flexibilities in mm/MN

In Table 3.3, results are presented per parameter in terms of flexibility (mm/MN).

PARAMETER	Huth equation	Grumman equation	3D benchmark flexibility	connector offset small elem	connector no offset small elem	connector offset large elem	connector no offset large elem	beam offset small elem	beam offset large elem
Plate material									
50000 MPa	29,25	36,72	34,82	86,56	39,28	82,32	39,04	45,68	43,31
72000 MPa	21,96	27,81	30,34	66,62	33,45	63,66	33,30	34,84	33,24
Bolt material									
72000 MPa	24,84	31,82	33,36	-	36,46	-	36,32	40,10	38,66
110300 MPa	21,96	27,81	30,34	66,62	33,45	63,66	33,30	34,84	33,24
210000 MPa	19,40	24,22	25,61	-	28,71	-	28,56	29,97	28,47
Plate thickness									
2.5 mm	27,85	43,15	45,78	112,54	52,14	101,02	51,90	49,73	46,15
5.1 mm	21,96	27,81	30,34	66,62	33,45	63,66	33,30	34,84	33,24
7.5 mm	19,31	30,10	29,17	43,38	31,29	42,38	31,18	36,51	35,45
Bolt diameter									
4 mm	25,48	35,00	36,82	75,58	39,97	72,62	39,82	43,46	41,89
5 mm	21,96	27,81	30,34	66,62	33,45	63,66	33,30	34,84	33,24
6.35 mm	18,73	23,95	24,26	-	-	-	-	29,50	-
7.93 mm	16,15	22,15	-	-	-	-	-	26,55	24,97
No of bolts									
1	21,96	27,81	-	-	-	-	-	27,82	26,59
2	21,96	27,81	30,34	66,62	33,45	63,66	33,30	34,84	33,24
3	21,96	27,81	28,00	-	33,45	-	33,33	32,06	30,50
Bolt spacing									
5D	21,96	27,81	30,34	66,62	33,45	63,66	33,30	34,84	33,24
8D	21,96	27,81	28,00	-	33,45	-	33,33	32,06	30,50
Plate width									
5D	21,96	27,81	30,34	66,62	33,45	63,66	33,30	34,84	33,24
10D	21,96	27,81	26,68	-	31,56	-	31,46	29,05	27,82

Table 3.3 – Flexibilities per parameter in mm/MN

These values are also visualized in Figure 3.3 to Figure 3.8.

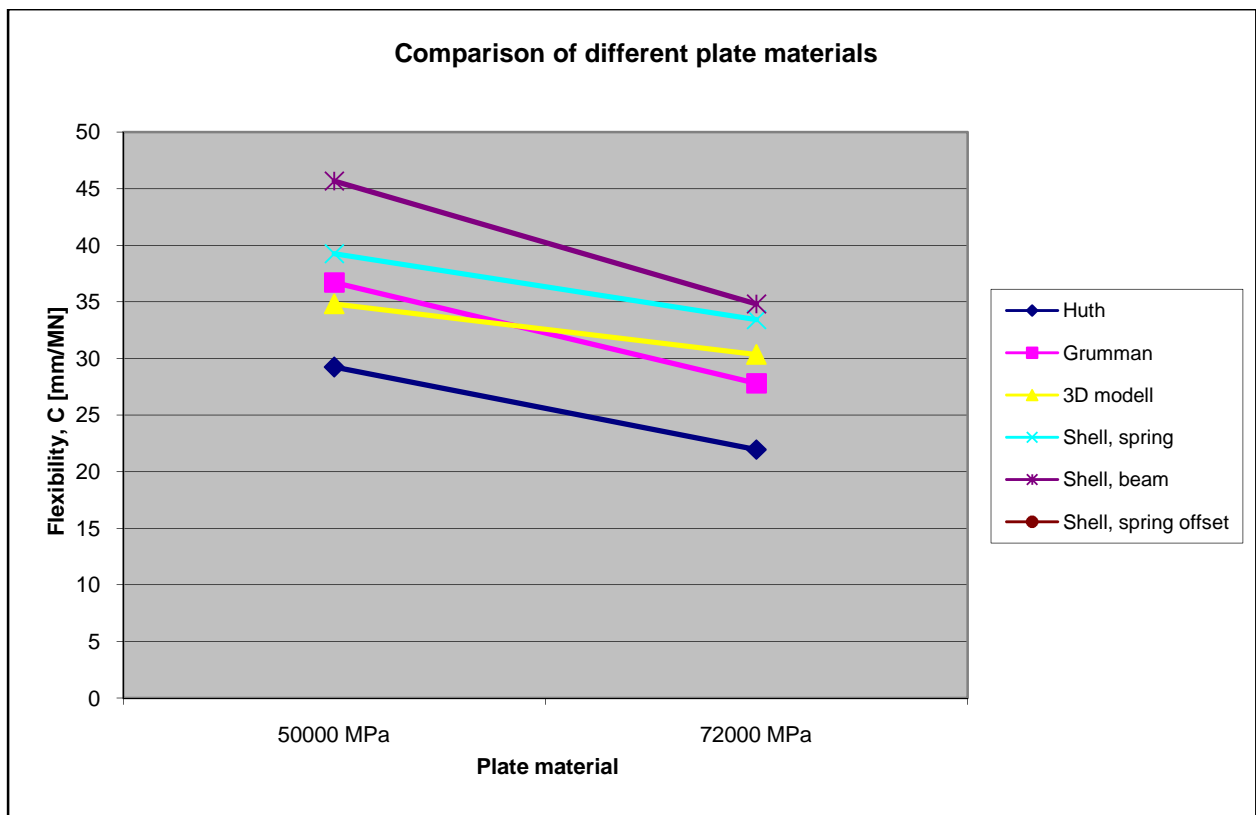


Figure 3.3 – Parameter: plate material

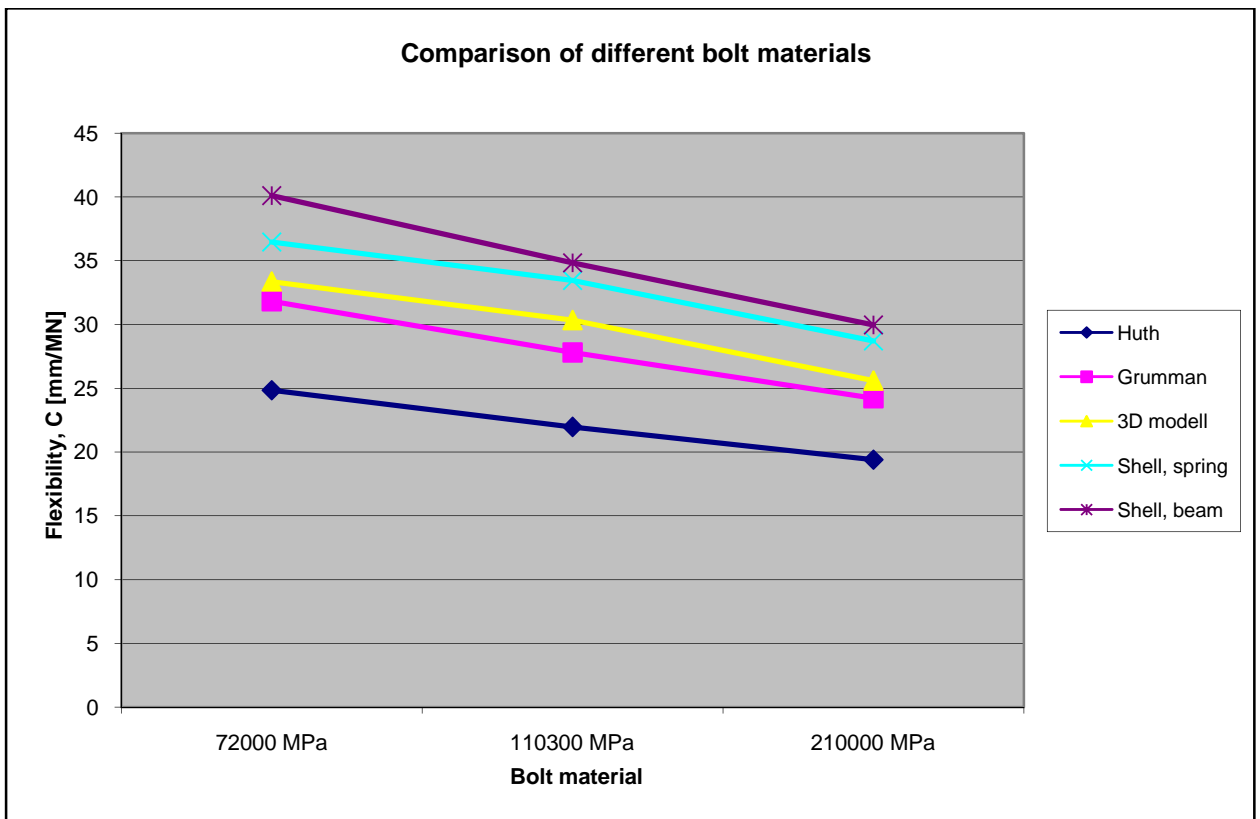


Figure 3.4 – Parameter: bolt material

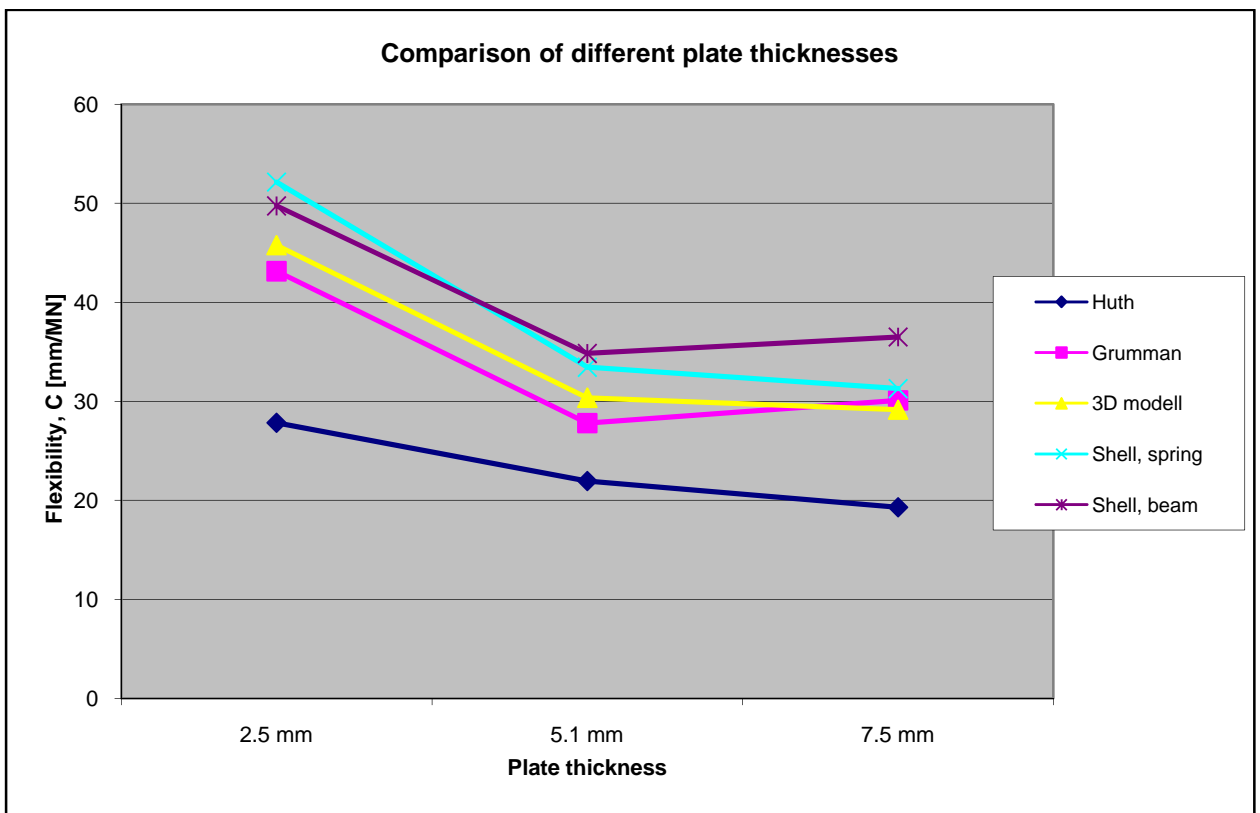


Figure 3.5 – Parameter: plate thickness

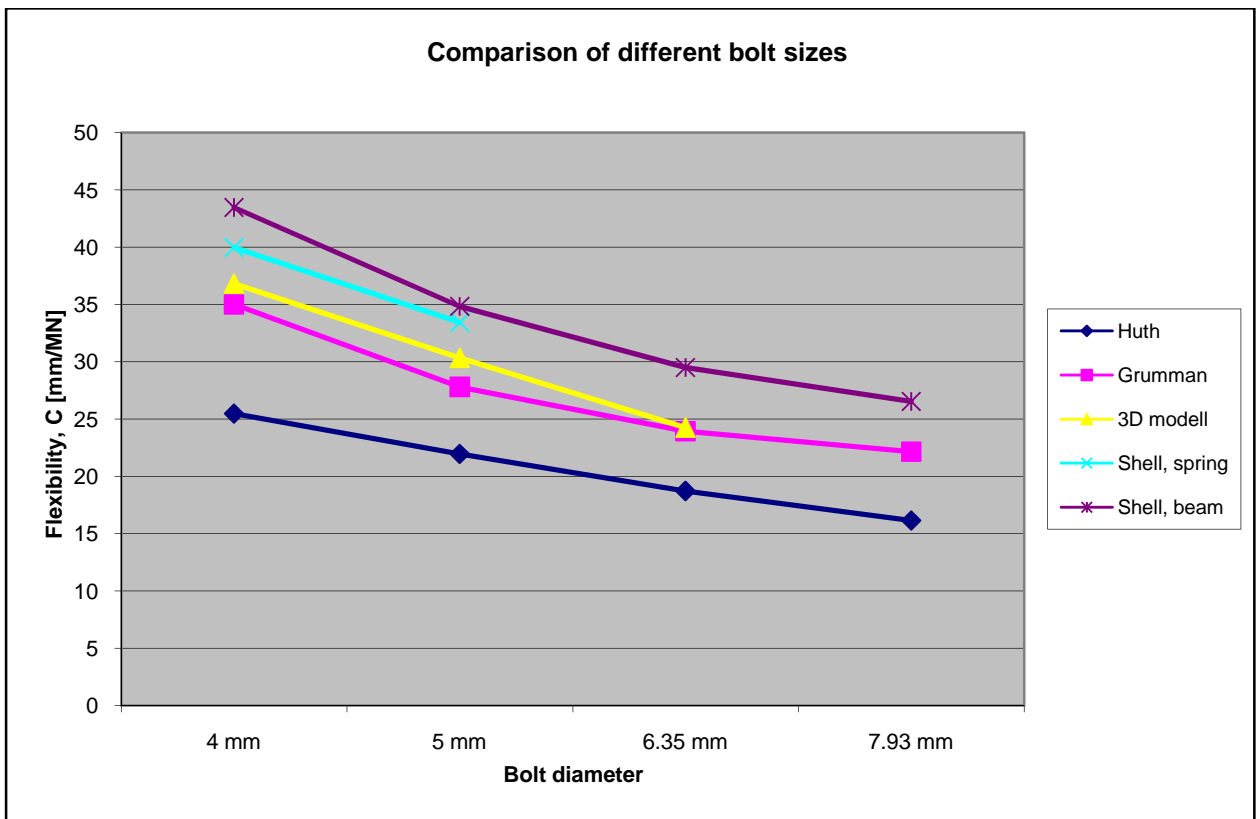


Figure 3.6 – Parameter: bolt size

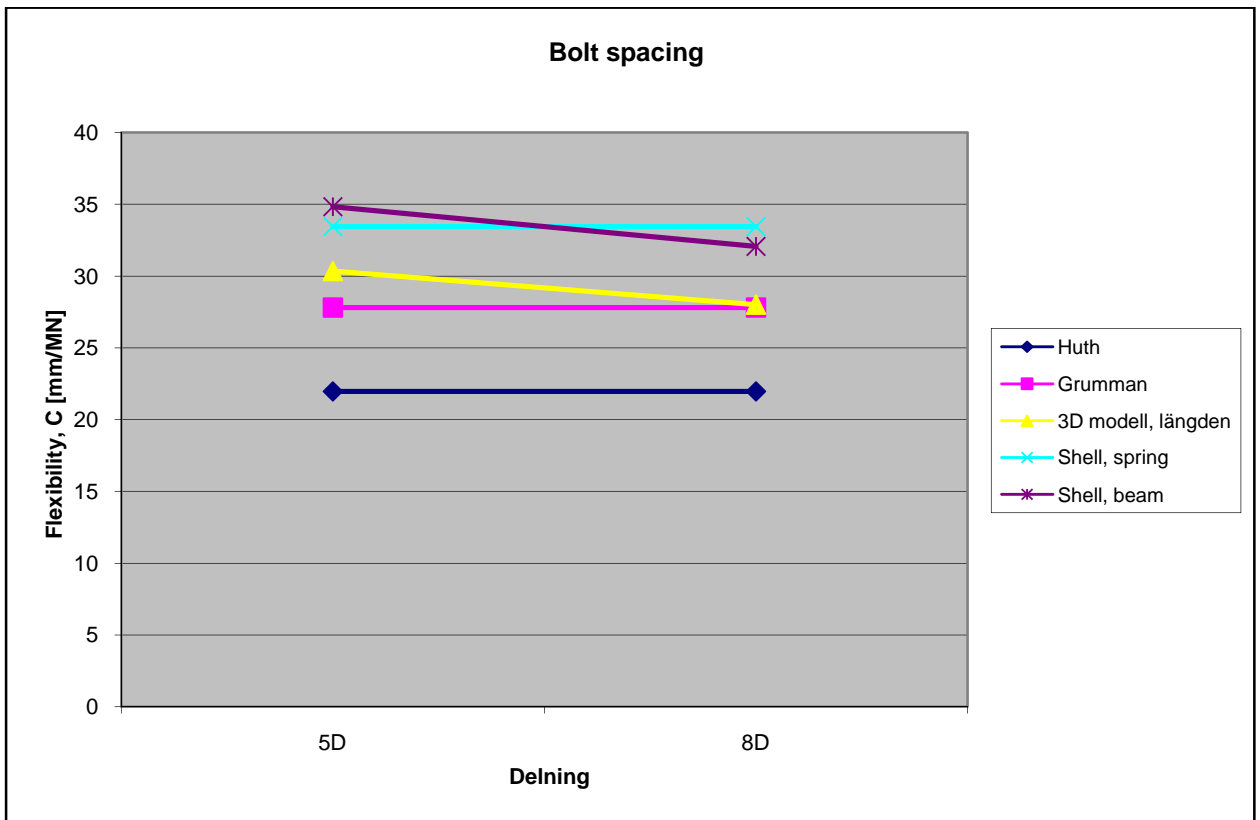


Figure 3.7 – Parameter: bolt spacing

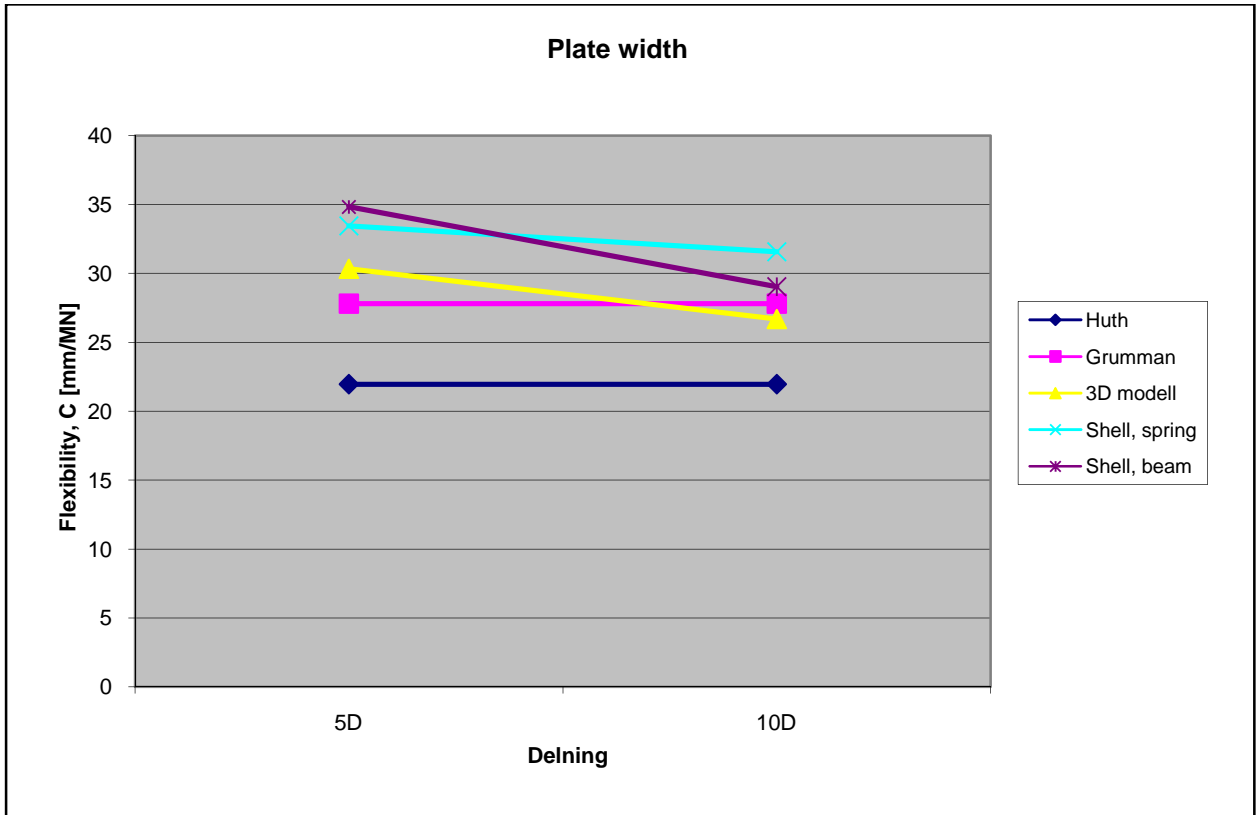


Figure 3.8 – Parameter: plate width

3.2.2 Load distribution in 3-bolted model

An important aspect when investigating simplified models is in this case the effect of using more bolts than two. In analysis number 13 in Table 3.1 three bolts are used. Looking at flexibility, the result seen in Table 3.2 seems to mirror its corresponding two bolt model relatively well when using the mean bolt value calculated below. The comparison of the 3D model with the 2D model indicates that the flexibility is higher in the middle bolt. But further evaluation is needed to determine the flexibility in each bolt.

$$\Delta l_{tot} = \frac{\delta_1 + \delta_2 + \delta_3}{3} + \Delta l_1 + \Delta l_2 + \Delta l_3 + \Delta l_4 \quad \text{Eq. 3.1}$$

$$\delta = \frac{\delta_1 + \delta_2 + \delta_3}{3} = \Delta l_{tot} - \Delta l_{elast} \quad \text{Eq. 3.2}$$

$$\Delta l_{elast} = \frac{P}{t_1 \cdot w \cdot E_1} \left(l_1 + \frac{l_2}{\frac{t_2 \cdot E_2}{t_1 \cdot E_1}} + \frac{l_3 + l_4}{1 + \frac{t_2 \cdot E_2}{t_1 \cdot E_1}} \right) \quad \text{Eq. 3.3}$$

The nodal forces are summed in the sections defined in Figure 3.9, and compared to the equivalent forces in the comparative beam shell model.

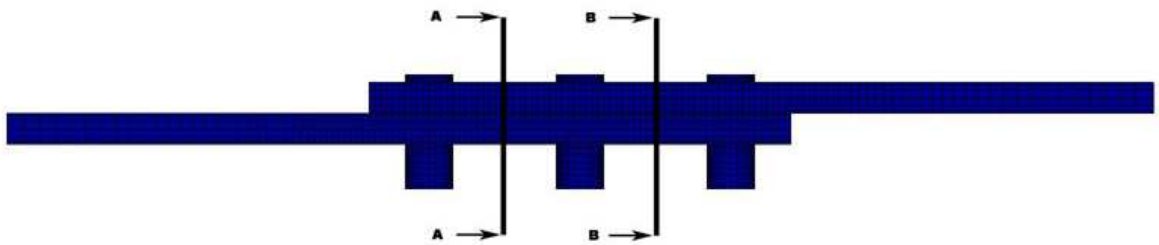


Figure 3.9 – Definition of sections in 3-bolted models

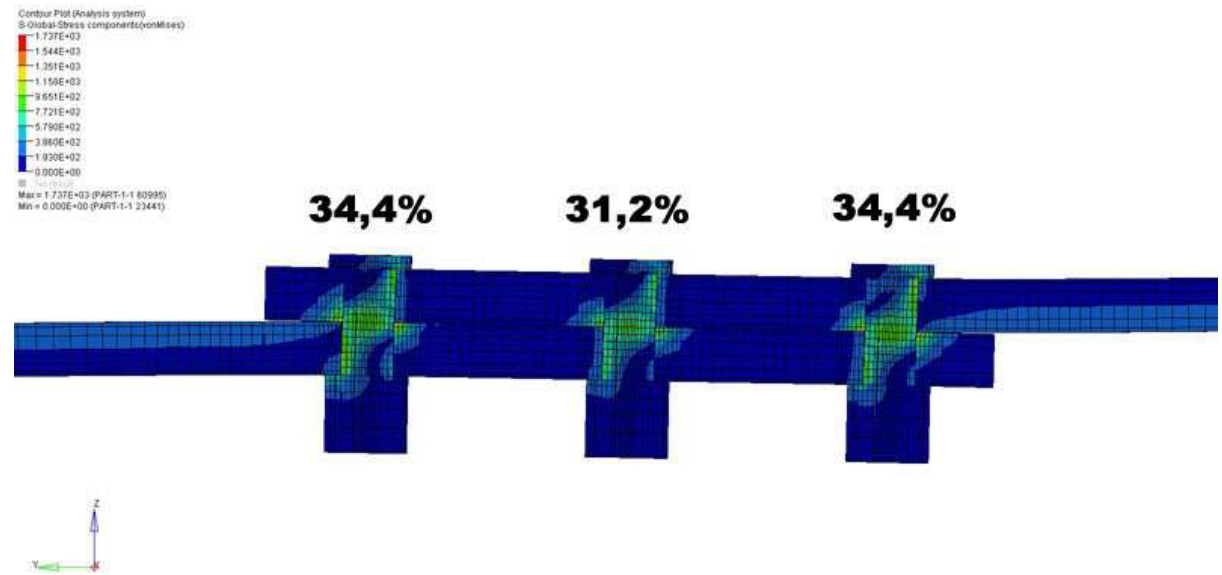


Figure 3.10 – Load distribution for 3-bolted 3D model

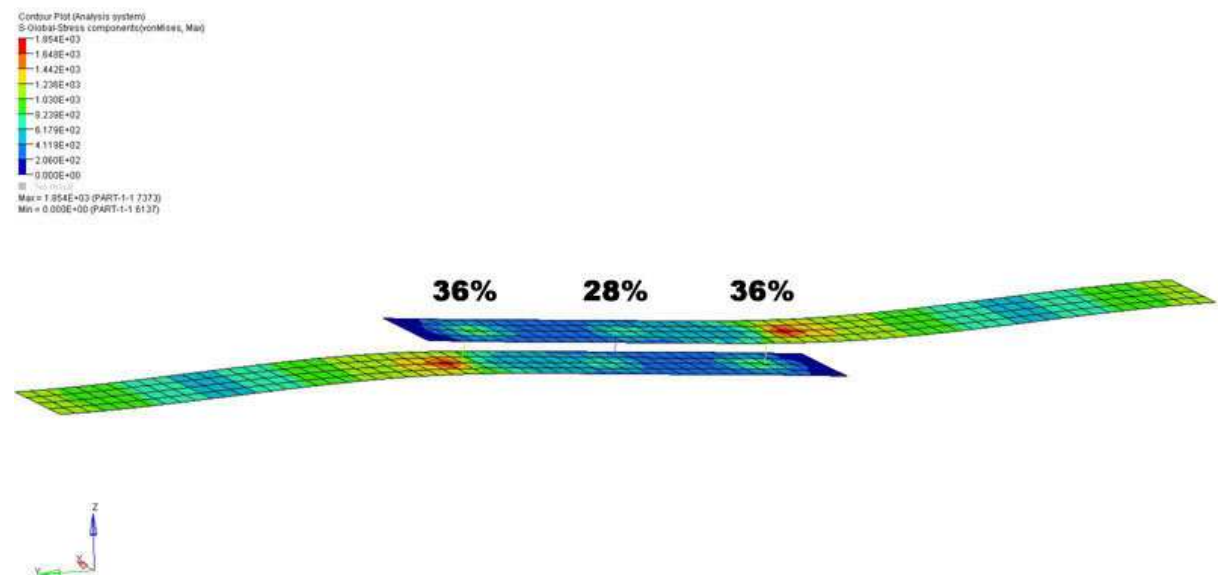


Figure 3.11 – Load distribution for 3-bolted shell model

Comparing Figure 3.10 and Figure 3.11, a difference in load distribution is highlighted between the three bolts in the 3D model and the beam elements used in the shell model.

3.3 Modifying factor for radius input

Using the knowledge of relatively constant difference in flexibility between the Grumman equation and the beam element method, a constant factor modifying the input radius reducing this error would increase overall accuracy for the model. A constant factor of 1.5 times the radius input in the ABAQUS input file was verified against Grumman for the reference analysis no. 2. As the error was no more than 1.3% in this case, further parameters were tested with the results in Table 3.4.

PARAMETER	Grumman equation	Unchanged radius input	50% increase of radius input	Difference unchanged vs Grumman	Difference 50% increase vs Grumman
Plate material					
50000 MPa	36,72	45,68	38,86	24,4%	5,8%
72000 MPa	27,81	34,84	28,17	25,3%	1,3%
Bolt material					
72000 MPa	31,82	40,10	30,22	26,0%	-5,0%
110300 MPa	27,81	34,84	28,17	25,3%	1,3%
210000 MPa	24,22	29,97	26,86	23,7%	10,9%
Plate thickness					
2.5 mm	43,15	49,73	47,38	15,3%	9,8%
5.1 mm	27,81	34,84	28,17	25,3%	1,3%
7.5 mm	30,10	36,51	24,07	21,3%	-20,0%
Bolt diameter					
4 mm	35,00	43,46	31,65	24,2%	-9,6%
5 mm	27,81	34,84	28,17	25,3%	1,3%
6.35 mm	23,95	29,50	25,84	23,2%	7,9%
7.93 mm	22,15	26,55	24,44	19,8%	10,3%

Table 3.4 – Constant scale factor of 1.5 for radius input (mm/MN)

These results are no improvement to the initial results when using original geometric data as input for the beam properties. Before the modification, values were ranging in between 15-20% from the target values. Thus, this factor does not give a more satisfactory result and should not be used.

It is obvious that a more complex modification is needed in order to improve accuracy of the model. By determining the parameters with most influence on the end result seen in Figure 3.12 and Figure 3.13, a formula for the scale factor may be found:

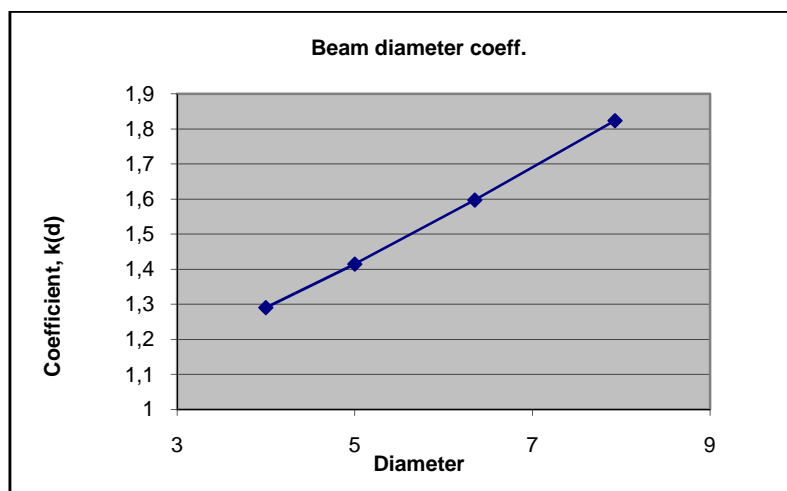


Figure 3.12 – Diameter function k(d)

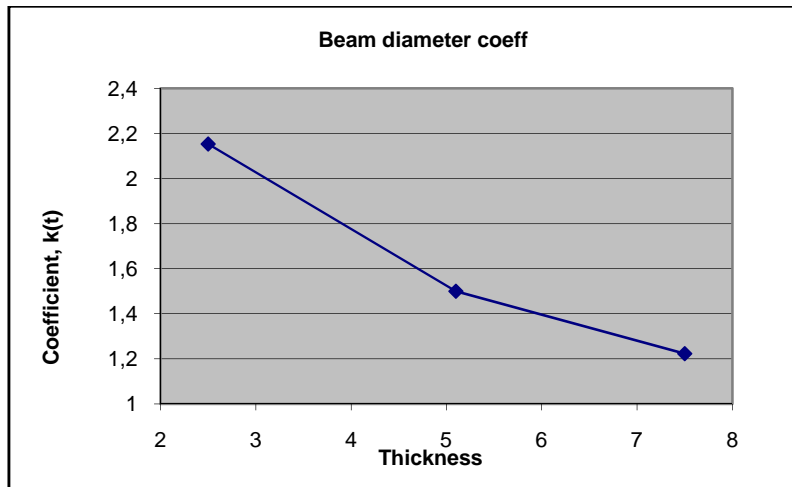


Figure 3.13 – Thickness function $k(t)$

$$k(d, t) = \frac{k(d) + k(t)}{2}$$

Eq. 3.4

$$k(d) = 0,13 \cdot d + 0,77$$

Eq. 3.5

$$k(t) = -0,19 \cdot t + 2,625$$

Eq. 3.6

$$\xrightarrow{yields} k(d, t) = 0,5 \cdot (0,13 \cdot d + 0,77) + 0,5 \cdot (-0,19 \cdot t + 2,625)$$

Eq. 3.7

$$\therefore k(d, t) = 0,065 \cdot d - 0,095 \cdot t + 1,6975$$

Eq. 3.8

This formula gives linear contribution from both the thickness and diameter to the scale factor for diameter input. Thus, the thickness input should be kept to its original value, only modifying the diameter input. A 3-dimensional presentation in Figure 3.14 gives an overview of the possible factors given a certain range of input data.

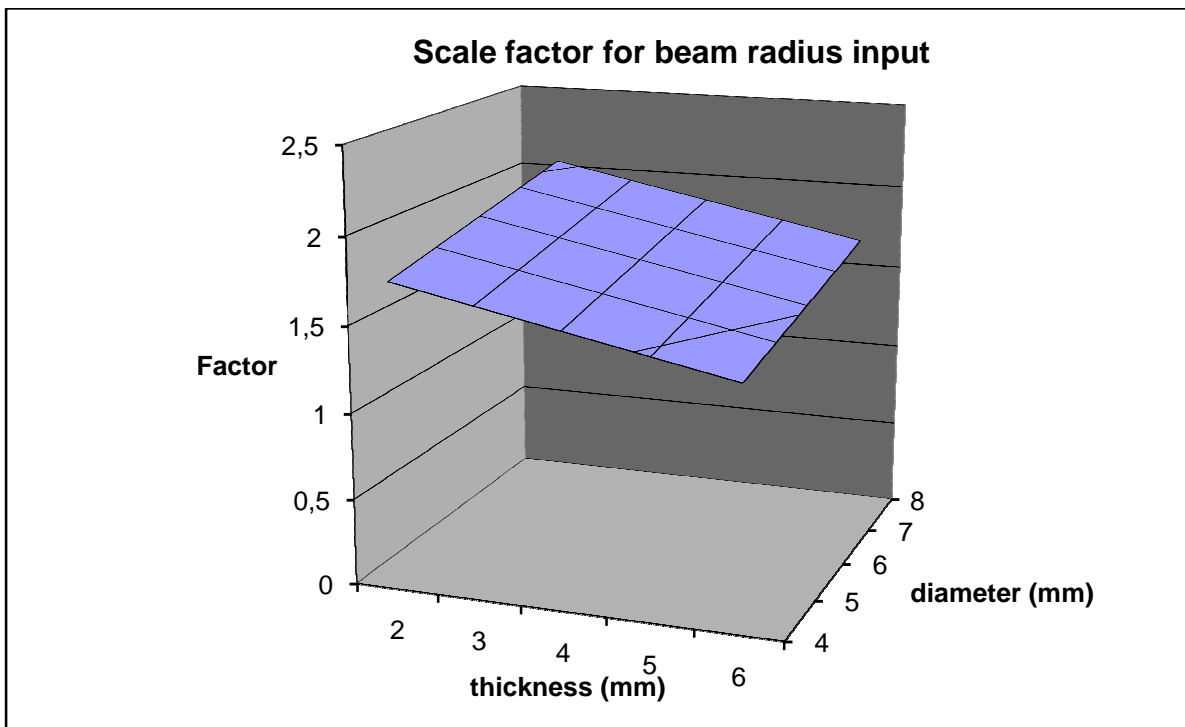


Figure 3.14 – Scale factor $k(d,t)$

Equation Eq. 3.8 is also verified in Table 3.5 with the Grumman formula (Eq. 2.12).

PARAMETER	Grumman equation	Scale factor modification	Difference
Plate material			
50000 MPa	36,72	38,62	5,2%
72000 MPa	27,81	28,17	1,3%
Bolt material			
72000 MPa	31,82	29,88	-6,1%
110300 MPa	27,81	28,17	1,3%
210000 MPa	24,22	26,21	8,2%
Plate thickness			
2.5 mm	43,15	46,88	8,7%
5.1 mm	27,81	28,17	1,3%
7.5 mm	30,10	26,81	-10,9%
Bolt diameter			
4 mm	35,00	31,86	-9,0%
5 mm	27,81	28,17	1,3%
6.35 mm	23,95	25,47	6,4%
7.93 mm	22,15	24,07	8,6%

Table 3.5 – Variable scale factor for radius input (mm/MN)

3.4 Interfacing with NASTRAN solver

Another option when using the spring element method is to use the NASTRAN solver. The FE model then needs to be converted to equivalent standard for this particular solver, the Bulk Data File. NASTRAN also uses a different name and description for spring elements. These are now called bushing elements, or CBUSH. Bushing elements are defined in a similar manner as the ABAQUS connector elements. They have three degrees of freedom for translations, with an optional three degrees for rotations. An important difference though is the lack of support for infinitesimal length of the actual element. This means in practice that when modelling without an offset, there still needs to be a small distance between the plates to avoid any singularities. Results are shown in Table 3.6.

Analysis no.	3D model (target)	ABAQUS model	NASTRAN model
2 (reference)	32954 N/mm	29898 N/mm	29713 N/mm

Table 3.6 – ABAQUS and NASTRAN shell model vs 3D model

4 Conclusions and Discussion

Modelling fasteners is concluded in Chapter 2.4 to be possible with a full 3D detailed study. Some factors are still unknown due to physical difficulties in measurement, but with the help of selected analyses this obstacle has been overcome and approximate values have been found.

The following notes give a good summary of performing detailed 3D analyses in terms bolt flexibility or simulations of shear loaded fastener installations:

- Eight-node brick elements works fine with a reasonable fine mesh. Variable mesh density is preferred to a fine density throughout the model.
- Contact modelling should be done with great care. A proper definition of the master and slave surfaces is crucial, see Figure 2.3.
- In order to get the true, non-linear behaviour of the lap-joint, material properties should be defined from stress-strain curves. If an aged lap-joint is to be modelled, using only the elastic material data is sufficient.
- Friction is best defined with a single value of static friction, if an initial state of the fastener is the objective of research. Otherwise it should be set to zero.
- The defining of pre-tension should reflect the objective of the analysis, as it may be done with either the initial or the minimum requirement for the specific bolt dimension.

The most preferred semi-empirical equation has proven to be the Grummel formula, see Chapter 3.2 and Table 3.3. It predicts the flexibility in good agreement with 3D FE models as well as experiments; see Figure 2.14 and Figure 2.17.

In FE analyses, the stress engineer has a couple of options when representing shear loaded fastener installations. When using shell elements through a load distribution analysis, two different methods have been validated for the ABAQUS/Standard solver, and one method for the NASTRAN solver.

For ABAQUS, the methods are based on the use of either beam elements (direct method), or connector element (two-step method). The beam element method only needs the input of known geometric and material data, e.g. diameter and modulus of the bolt. A requirement is though that the connecting nodes need to be in the exact position of the bolt as well as orthogonal to each other. This is because BAR2 elements use a local orientation domain when applying stiffness properties. Compared to a benchmark 3D detailed model, this representation lies constantly around 15-20% above in terms of flexibility, which is a relatively good result. Also, with this in mind, proper adjustments may be possible in order to get an even more accurate fastener representation. An equation (Eq. 3.8) to modify the beam diameter in the FE analysis has also been presented in Chapter 3.3, where the input radius of the beam element is altered because of this reason. Either way with or without modifying the input data, using the beam element method always (given that only thin structures are modelled with shell elements in their mean surface) gives a reasonable representation.

$$k(d, t) = 0,065 \cdot d - 0,095 \cdot t + 1,6975$$

Eq. 3.8

A different approach is the method of using springs, usually called connector elements in ABAQUS, to represent the fastener. Since springs do not make use of any geometric data, the inputs are stiffnesses in each degree of freedom. This means a pre-analysis calculation needs to be done prior to the main analysis, i.e. either a detailed 3D study or an analytical approach with one (or more) formula normally used in the industry, see Chapter 2.3. Just as with a beam element, the nodes in the meshed shell structure needs to be situated in the exact position of the fastener installation. The reward for using this method, which obviously requires more work, is a slightly better accuracy in terms of flexibility. It has also been proven in Chapter 3.4 that this method works just as well with the NASTRAN solver and its connector element equivalent called bushing elements. An important notice for this method is the awareness of stiffness value origin. Technically, the spring element models may be modelled with or without an offset between the plates. This may be a choice of great importance, since offset induce secondary bending while using no offset does not. Some methods of finding appropriate spring stiffness already take this effect into account, e.g. Grumman formula and the detailed 3D model. Fasteners should therefore be modelled **without an offset** when using values from these origins, otherwise secondary bending will be taken into account twice as a total in the analysis. This has proven by the results in Table 3.2 in Chapter 3.2 to be erroneous.

The morphing technique (see Chapter 2.1) is proven to work very well for the purpose of detailed 3D modelling and when large amounts of models are generated. It is therefore recommended for use when performing large parametric studies.

4.1 Recommendations and guidelines

Finally, guidelines for prediction and modelling fastener flexibility in load distribution analysis are summarized.

- When determining flexibility using 3D FE analysis
 - Use no friction.
 - Use no plasticity.
 - Use a pre-tension equal to a minimum requirement.
- Use the Grumman equation if flexibility is determined with empirical equation.
- If load distribution model is modelled with an offset (mid-plane of joined parts)
 - Use beam elements with circular cross-section for fasteners.
 - Use actual fastener diameter or diameter multiplied with scale factor determined with Eq. 3.8.
- If load distribution model is modelled without offset (joined parts in same plane)
 - In ABAQUS, use Cartesian connector element and in NASTRAN, bush elements.
 - Determine fastener flexibility with Grumman equation or detailed 3D FE analysis.

5 Further work

The work may be extended in the following directions:

- Further verification with NASTRAN solver: full parametric study for CBUSH element as well as with an appropriate beam element.
- A non-linear scale factor equation $k(d,t)$, and possibly incorporating material parameters in the equation as variables, $k(d,t,E_b,E_p)$. This operation would need even further analyses with benchmark values in order to build a smooth curve.
- Investigate interaction with other load cases, e.g. tension loaded bolts or shear loaded in different direction.
- Verify both the 3D model as well as shell models for larger installations, four bolts or more, in terms of flexibility and load distribution.

References

- ABAQUS 6.7-1 Keywords Reference.* DDS Simulia.
- Austin, M. (2004). *Bolt flexibilities from ESDU Data Items 85034 and 98012.* Airbus-UK.
- Beardmore, R. (2007, 05 07). *RoyMech.* Retrieved 10 09, 2007, from http://www.roymech.co.uk/Useful_Tables/Tribology/co_of_frict.htm
- Huckcomp. *Qualification Test Results LGP Composite Fastening System.* Report Huckcomp 84LGP9-120.
- Huckcomp (1991). *Creep Measurement of Clamp Force on Huckcomp/Lightweight GP/Hi-Lite Fasteners.* Report Huckcomp TCT-90-8.
- Huth, H. (1983). *Experimental determination of fastener flexibilities.* Report LBF-Bericht nr. 4980. Fraunhofer-Institut für Betriebsfestigkeit, Darmstadt, 9 pp.
- Huth, H. (1984). *Zum Einfluss der Nietnachgiebigkeit mehrriger Nietverbindungen auf die Lastübertragungs- und Lebensdauervorhersage.* Report Bericht FB-172. Fraunhofer-Institut für Betriebsfestigkeit, Darmstadt, 76 pp.
- HyperWorks HyperMesh 8.0sr1 User's Manual.* Altair Engineering.
- Jarfall, L. (1983). *Shear loaded fastener installations.* Report SAAB KH R-3360. Aircraft Division Saab-Scania AB, Linköping, 68 pp.
- MIL-HDBK-5E. *Military Handbook.*
- MMPDS-02. *Metallic Materials Properties Development and Standardization.*
- Olert, M. (2004). *Load Redistribution in Bolted Joints due to Composite Damage and Metal Plasticity.* Report LiTH-IKP-Ex-2145. Department of Mechanical Engineering, Linköping University, Linköping, 65 pp.
- Palmberg, B. (1986). *Fatigue life and fastener flexibility of single shear joints with countersunk fasteners.* Report FFA TN 1986-01. The Aeronautical Research Institute of Sweden, Stockholm, 71 pp.
- Ramsdale, R. (2007). *Engineer's Handbook.* Retrieved 10 10, 2007, from <http://www.engineershandbook.com/Tables/frictioncoefficients.htm>
- Segerfröjd, G. (1995). *Fatigue in Mechanical Joints - A Literature Survey.* Report FFA TN 1993-56. The Aeronautical Research Institute of Sweden, Stockholm, 94 pp.
- Södergren, L., & Lundahl, Ö. (1986). *Tillvägagångsätt vid framtagning av flexibilitetsdata till Strength Data.* Report SAAB TKH R-3463. Aircraft Division Saab-Scania AB, Linköping, 5 pp.